npj Parkinson's Disease

https://doi.org/10.1038/s41531-025-01225-3

Article in Press

Backtracking α-synuclein pathology: social deficits precede motor symptoms in Parkinson's disease

Received: 16 June 2025

Accepted: 19 November 2025

Cite this article as: Marino, G., Campanelli, F., Natale, G. *et al.* Backtracking α-synuclein pathology: social deficits precede motor symptoms in Parkinson's disease. *npj Parkinsons Dis.* (2025). https://doi.org/10.1038/s41531-025-01225-3

Gioia Marino, Federica Campanelli, Giuseppina Natale, Maria De Carluccio, Federica Servillo, Sofia Nutarelli, Maria Emiliana Caristo, Maria Teresa Viscomi, Veronica Ghiglieri & Paolo Calabresi

We are providing an unedited version of this manuscript to give early access to its findings. Before final publication, the manuscript will undergo further editing. Please note there may be errors present which affect the content, and all legal disclaimers apply.

If this paper is publishing under a Transparent Peer Review model then Peer Review reports will publish with the final article.

ARTICLE IN PRESS

© The Author(s) 2025. **Open Access** This article is licensed under a Creative Commons Attribution-NonCommercial-NoDerivatives 4.0 International License, which permits any non-commercial use, sharing, distribution and reproduction in any medium or format, as long as you give appropriate credit to the original author(s) and the source, provide a link to the Creative Commons licence, and indicate if you modified the licensed material. You do not have permission under this licence to share adapted material derived from this article or parts of it. The images or other third party material in this article are included in the article's Creative Commons licence, unless indicated otherwise in a credit line to the material. If material is not included in the article's Creative Commons licence and your intended use is not permitted by statutory regulation or exceeds the permitted use, you will need to obtain permission directly from the copyright holder. To view a copy of this licence, visit http://creativecommons.org/licenses/by-nc-nd/4.0/.

ARTICLE IN PRESS

Backtracking α-synuclein pathology: social deficits precede motor symptoms in Parkinson's Disease

Gioia Marino[1*]; Federica Campanelli[2*]; Giuseppina Natale[2]; Maria De Carluccio[3]; Federica Servillo[3]; Sofia Nutarelli[4]; Maria Emiliana Caristo[5]; Maria Teresa Viscomi[1,4]; Veronica Ghiglieri[1,2+]; Paolo Calabresi[1,3+#]

1. *Fondazione Policlinico Universitario Agostino Gemelli IRCCS, Rome, Italy*
2. *Dipartimento di Scienze Umane e Promozione della Qualità della Vita, Università Telematica San Raffaele, Rome, Italy.*
3. *Dipartimento di Neuroscienze, Università Cattolica del Sacro Cuore, Neurologia, Rome, Italy*
4. *Dipartimento di Scienze della Vita e Sanità Pubblica, Università Cattolica del Sacro Cuore, Rome, 00168, Italy.*
5. *Cen.Ri.S. Policlinico Gemelli UNICATT, Rome, Italy.*

*These authors contributed equally to this work.

+These authors contributed equally to this work.

#Correspondence should be addressed to:

Prof Paolo Calabresi, MD
Direttore Clinica Neurologica,
Dipartimento di Neuroscienze,
Facoltà di Medicina e Chirurgia,
Università Cattolica del Sacro Cuore,
Largo Francesco Vito 1, 00168,
Roma, Italia
Phone: +39 06 30154459
Email: paolo.calabresi@policlinicogemelli.it

Keywords: Alpha-synuclein, ventral striatum, synaptic plasticity, cognition, premotor PD

Word count

Number of words in the abstract: 212
Number of words in the main manuscript: 8837
Number of figures/tables: 7, plus 2 supplementary
References: 70

ARTICLE IN PRESS

ARTICLE IN PRESS

ARTICLE IN PRESS

ARTICLE IN PRESS

Abstract

In Parkinson's disease (PD), degeneration of dopaminergic neurons in the substantia nigra pars compacta and accumulation of alpha-synuclein (α-syn) aggregates are linked to motor impairments. However, up to 80% of PD patients also experience cognitive and psychiatric issues. The effects of α-syn aggregates on limbic structures involved in social behavior are less studied. Here, we hypothesize that early synaptic changes in the mesolimbic dopaminergic system occur before motor symptoms, affecting social cognition (SC). Four weeks after intrastriatal injections of human-α-syn pre-formed fibrils, at a pre-motor stage, dorsolateral striatum plasticity remains intact, while long-term potentiation in the Nucleus Accumbens (NAc)-Core is lost, correlating with deficits in SC and spatial memory. Reduced dopaminergic and glutamatergic inputs and decreased dendritic spine density were also observed. Sub-chronic L-Dopa treatment reversed these changes. Our data suggest that SC is affected early in this synucleinopathy, with synaptic alterations in the NAc-Core playing a key role.

ARTICLE IN PRESS

ARTICLE IN PRESS

Introduction

Parkinson's disease (PD) is the second-most common neurodegenerative disorder [1]. Neuronal loss in the substantia nigra pars compacta (SNpc), which causes striatal dopamine (DA) deficiency, and intracellular inclusions containing aggregates of α-synuclein (α-syn) are the pathological hallmarks of PD [2,3]. Although motor signs such as tremor, rigidity, and bradykinesia are the key characteristics of the disease, cognitive impairment is an important non-motor feature in PD, and the spreading of α-syn in specific brain areas is an important mechanism of early cognitive impairment in this disease [3,4]. Recently, significant correlations between impairment in social cognition (SC), a cognitive domain that allows one to understand others' intentions and to regulate behavior in social contexts, and memory dysfunctions were reported in parkinsonian patients [5,6].

Clinical studies have recently shown that patients with movement disorders exhibit selective difficulties in SC [7–10]. Findings investigating SC in various hypo- and hyper-kinetic movement disorders (in particular PD) revealed a critical contribution of the basal ganglia in the pathological impairment of SC, even in the early phases of the disease[11]. Thus, although these nuclei (caudate, putamen, globus pallidus, substantia nigra) and fronto-striatal circuits, also involving the cortex and thalamus, were classically implicated in critical motor functions [12], new experimental and clinical observations reported a key contribution of the basal ganglia also in cognitive domains, and in particular in SC.

At this point, key neurobiological and clinical questions arise: i) How do the dopaminergic pathways contribute to SC in healthy subjects? ii) Which brain structures, in addition to the basal ganglia, are implicated in the SC dysfunctions observed in early PD patients showing only a mild dopaminergic denervation? iii) Does sub-chronic L-3,4-dihydroxyphenylalanine (L-Dopa) restore the SC deficits in the early stage of the disease? [13,14]. Unfortunately, most of the current findings are conflicting and fail to identify a clear synaptic mechanism and a specific brain area mediating these social deficits.

Interestingly, experimental results suggest that, among the different dopaminergic circuits, physiological and pathological conditions affecting social behavior are specifically mediated by nucleus accumbens (NAc) activity [15,16]. Recently, a large cohort study found that loneliness and social isolation are associated with the risk of PD. Moreover, SC changes can alter social functioning, thus leading to further social withdrawal. Social withdrawal may result in adverse

ARTICLE IN PRESS

outcomes for PD patients, influencing their quality of life [17]. Thus, it is important to reveal the neurobiological contribution of SC in PD to develop strategies to face this clinical problem and prevent its negative outcomes.

Here, we addressed the specific role of DA in regulating social and cognitive behaviors by NAc in an α-syn-based model of early PD [18,19]. We found that in rats injected with intrastriatal pre-formed fibrils (PFF) of human α-syn, in the early stage of progression, synaptic plasticity in the dorsal striatum was not altered, in line with the absence of motor deficits. Conversely, at the same time point, in the spiny projection neurons (SPNs) recorded from NAc-Core, long-term potentiation (LTP) was impaired, and SC disturbances and visuo-spatial cognition paralleled this synaptic alteration. Interestingly, dopaminergic input from the ventral tegmental area (VTA) was also reduced. We also found structural plasticity alterations in the dendritic spine density of ventral striatum SPNs.

Our findings strongly suggest that the early synucleinopathy causes a premotor stage in which mild dopaminergic denervation in the ventral striatum is sufficient to trigger SC deficit and synaptic plasticity changes before subtle motor symptoms associated with dorsolateral striatum synaptic alterations appear. Our results provide a novel mechanistic view in which VTA-NAc dopaminergic projection impairment causes SC deficits.

ARTICLE IN PRESS

Results

Injection of α-syn-PFFs triggers early loss of DA terminals in the NAc-Core but not in the dorsolateral striatum (STR-DL)

Based on the previously reported effects of striatal α-syn PFFs injection on the nigrostriatal dopaminergic terminals [18], we analyzed the outcome at the earliest time point, 4 weeks after the lesion (Fig. 1A). We performed a TH^+ immunofluorescence in the dorsolateral striatum (STR-DL), and no difference was observed between PBS and α-syn-PFFs–injected rats (Fig. 1B; Mann-Whitney's t-test, PBS n = 5 *versus* PFF n = 7, U = 12, P > 0.05). To further explore the functional integrity of dopaminergic presynaptic terminals, we analyzed the immunostaining intensity of striatal DA active transporter (DAT) in the STR-DL. Also in this case, no significant differences were detected between the two experimental groups (Fig. 1B; Mann-Whitney's t-test, PBS n = 5 *versus* PFF n = 8, U = 18, P > 0.05). We then performed the same immunofluorescence analyses in the NAc-Core, and, interestingly, in α-syn-PFFs–injected rats we observed a significant reduction in the optical density of TH^+ terminals (Fig. 1C; Mann-Whitney's t-test, PBS n = 6 *versus* PFF n = 7, U = 2, **P < 0.01) and DAT^+ fibers compared to the PBS group (Fig. 1C; Mann-Whitney's t-test, PBS n = 5 *versus* PFF n = 6, U = 0, **P < 0.01).

A single intracerebral injection of PFFs is sufficient to induce the misfolding and aggregation of endogenous α-syn in recipient neurons and its subsequent spreading through anatomically and functionally connected neuronal circuits[20]. Given the propensity of α-syn-PFFs to spread through the nigrostriatal pathway [18,21], we measured the immunostaining intensity of a pathological form of α-syn, phosphorylated at the Ser^{129} residue (p129-αSyn), in the midbrain areas VTA and SNpc, as well as in the NAc-Core and STR-DL. Four weeks after the injection, α-syn-PFFs were detected in the STR-DL (Fig. 1B; Mann-Whitney's t-test, PBS n = 7 *versus* PFF n = 7, U = 6, *P < 0.05) with even more pronounced spread in the NAc-Core (Fig. 1C; Mann-Whitney's t-test, PBS n = 7 *versus* PFF n = 8, U = 3, **P < 0.01). Surprisingly, no differences between PFF- and PBS-injected rats were observed in the SNpc (Fig. 1D; Mann-Whitney's t-test, PBS n = 5 *versus* PFF n = 6, U = 7, P > 0.05) and in the VTA (Fig. 1E; Mann-Whitney's t-test, PBS n = 6 *versus* PFF n = 6, U = 1, P > 0.05). Additionally, α-syn-PFF spreading assays have been performed in the motor cortex M1 and the dorsomedial striatum (STR-DM). In both areas, we found a significant increase of α-syn aggregates compared to controls (Supplementary Fig. 1A-B; Mann-Whitney's t-test, motor

cortex: PBS n = 8 *versus* PFF n = 8, U = 7, **P < 0.01; STR-DM: PBS n = 8 *versus* PFF n = 7, U = 1, ***P < 0.001). In line with the large amount of α-syn-PFF in the STR-DM, a significant neurodegeneration of the terminals has been observed, as detailed in the data regarding TH^+ and DAT^+ fibers (Supplementary Fig. 1B; Mann-Whitney's t-test, TH: PBS n = 5 *versus* PFF n = 5, U = 0, **P < 0.01; DAT: PBS n = 5 *versus* PFF n = 5, U = 0, **P < 0.01). Considering the obtained data, we performed an unbiased stereological analysis of TH^+ neurons to determine the extent of dopaminergic neuronal loss in the SNpc and VTA that project to STR-DL and NAc-Core, respectively. In both brain areas analyzed, no significant differences were observed between PBS rats and those injected with α-syn-PFFs (Fig. 1F; Mann-Whitney's t-test, SNpc, PBS n = 5 *versus* PFF n = 6: left bar dots graph, U = 12, P > 0.05; VTA, PBS n = 6 *versus* PFF n = 6: right bar dots graph, U = 13, P > 0.05).

Injection with α-syn-PFFs causes social cognition impairments before motor deficits

Four weeks after the injection of α-syn aggregates, animals were subjected to motor and social interaction tests to investigate the effects of PFF aggregates.

To identify if this latency after the lesion could be the earliest timepoint of motor impairment caused by α-syn-PFF, we subjected the rats to grid walking and Rotarod tests (Fig. 2A-B). In the grid walking test, the α-syn-PFF animals (n = 13) showed motor performances similar to those observed in PBS (n = 12). In particular, we found no change in the motor parameters such as the time to the top (Mann-Whitney's t test; PBS *versus* PFF, U = 34, P > 0.05), the rotation time (Mann-Whitney's t test; PBS *versus* PFF, U = 71, P > 0.05), the number of the cross (Mann-Whitney's t test; PBS *versus* PFF, U = 66, P > 0.05) and the immobility time (Mann-Whitney's t test; PBS *versus* PFF, U = 12, P > 0.05). To further detect possible motor deficits, experimental groups were subjected to a Rotarod test with an incremental motor learning paradigm, a complex test requiring motor learning and coordination. Also in this condition, PBS (n = 5) and PFF (n = 4) groups learned the task similarly, showing a constant and comparable latency to fall, across days (Fig. 2B; Two-way ANOVA, interaction, $F_{(2,14)} = 0.045$, P > 0.05 and group, $F_{(1,7)} = 0.157$, P > 0.05; Bonferroni's post hoc test).

Since deficits in social interaction have been reported in early PD patients, we decided to explore this cognitive domain in our premotor model of synucleinopathy. Firstly, to evaluate anhedonia-like behavior in our early model, animals were subjected to sucrose preference test, which reflects the animal's sensitivity to natural rewards. Our results showed that PFF rats (n = 6) did not exhibit a significant reduction in sucrose consumption compared to PBS animals (n = 6), indicating that at this time point injection of α-syn-PFFs did not impair motivation or reduce interest in rewarding stimuli (Fig. 3A, One way ANOVA; PBS *versus* PFF, Day 1: $F_{(3,20)} = 1.29$, Bonferroni's post hoc test, t = 1.55, df = 20, P > 0.05; Day 2: $F_{(3,20)} = 2.42$, Bonferroni's post hoc test, t = 1.77, df = 20, P > 0.05).

Then, we examined potential changes caused by α-syn-PFFs injection during the free-social interaction test, measuring the contact duration under two conditions. In the first condition, we assessed the animal's interaction with an inanimate object. In the second condition, social behavior was tested with a stimulus rat (conspecific). During the session with the inanimate object, we found no difference in the time spent exploring the object between the PFF (n = 8) and PBS (n = 5) groups (Fig. 3B; Mann-Whitney's t test; PBS *versus* PFF, U = 16, P > 0.05). Conversely, during the social interaction session, we observed a lower ability of α-syn-PFF rats to approach and explore the conspecific animal (Fig. 3B; Mann-Whitney's t test; PBS *versus* PFF, U = 0, **P < 0.01). These findings are in agreement with the literature showing that patients in the early stages of PD have cognitive deficits, including difficulty in interpreting social signals and maintaining interpersonal relationships [7]. To confirm this data, we employed the three-chamber test to evaluate both sociability and social novelty preferences. As expected, PBS rats (n = 6) showed a significant preference for the social target (ST) during the sociability session (Fig. 3C, left,; One way ANOVA, $F_{(4,20)} = 19.52$, Bonferroni's post hoc test, t = 6.11, df = 20, PBS: ST *versus* E, ***P < 0.0001), and a preference for the novel target (NT) over the familiar target (FT), during the social novelty session (Fig. 3C, right; One way ANOVA, $F_{(4,20)} = 7.57$, Bonferroni's post hoc test, t = 3.22, df = 20, PBS: NT *versus* FT, *P < 0.05). In contrast, PFF rats (n = 6), 4 week after the lesion, exhibit a significant deficit in sociability (Fig. 3C, left; One way ANOVA, $F_{(4,20)} = 19.52$, Bonferroni's post hoc test, t = 1.48, df = 20, PFF: ST *versus* E, *ns*, P > 0.05) and social novelty (Fig. 3C, right; One way ANOVA, $F_{(4,20)} = 7.57$, Bonferroni's post hoc test, t = 0.70, df = 20, PFF: NT *versus* FT, *ns*, P > 0.05) compared to the control group (PBS) (sociability: PBS *versus* PFF, $F_{(4,20)} = 19.52$, Bonferroni's post hoc test, t = 6.15, df = 20, ***P < 0.0001; social novelty: PBS

versus PFF, $F_{(4,20)} = 7.57$, Bonferroni's post hoc test, t = 4.93, df = 20, ***P < 0.001), with no preference for the ST and NT. No sign of reduced locomotion during the three-chamber test was observed in PFF rats.

To assess anxiety behavior and locomotion, 4 weeks after the injection, rats were subjected to the open field task (Fig. 3D). The statistical comparison between PFF (n = 7) and PBS (n = 8) groups showed no difference in all the evaluated parameters. In particular, α-syn-PFF–injected rats did not show a reduction in exploration of the center arena compared to control animals (Fig. 3D; Two-way ANOVA, $F_{(1,26)} = 0.11$, Bonferroni's post hoc test, PBS versus PFF: P = 0.74), suggesting that α-syn pathology at this time point does not induce anxiety-like behavior. The PFF rats behave similarly to the control animals, with a similar exploratory behavior and a natural decreased distance traveled (Fig. 3D; Two-way ANOVA, $F_{(1,26)} = 39.41$, Bonferroni's post hoc test, PBS: **P < 0.01 ; PFF: ***P < 0.001) and mean speed in the last 5 minutes (5'- 10') (Fig. 3D; Two way ANOVA, $F_{(1,26)} = 59.82$, Bonferroni's post hoc test, PBS and PFF ***P < 0.001). An increase in the immobility time between the first 5 (1'- 5') and following 5 min (5'- 10') was observed in both PBS- and PFF-injected animals with significance in PD rats (Fig. 3D; Two-way ANOVA, $F_{(1,22)} = 16.70$, Bonferroni's post hoc test, **P < 0.01), even if not associated with motor clinical signs.

Finally, in the modified object recognition test we observed that PBS (n = 8) and PFF (n = 8) groups similarly explored all objects placed in the arena during the habituation phase (sessions 2 to 7) (Fig. 3E; left: Two-way ANOVA: interaction time x group, $F_{(5,35)} = 0.902$, P = 0.491, Bonferroni's post hoc test). During session 8 (S8), when one object was moved to a different part of the arena, the spatial change of this object (displaced object, DO) was detected by PBS animals that prefer to explore DO compared to non-displaced objects (NDOs) (Fig. 3E; right: Two-way ANOVA: interaction, $F_{(1,14)} = 421.5$; Bonferroni's post hoc test, ***P < 0.001). Interestingly, we found that α-syn-PFFs-injected rats explored DO and NDOs equally, indicating a deficit in spatial discrimination (Fig. 3E; P = 0.214).

Long-term potentiation in SPNs of NAc-Core, but not in STR-DL neurons, is precociously impaired by α-syn-PFFs

ARTICLE IN PRESS

To investigate the effects of α-syn-PFFs injection on the striatal neuronal activity, SPNs of STR-DL, from PBS (n = 6) and PFF (n = 7) rats, were recorded through *ex vivo* patch-clamp and intracellular techniques, 4 weeks after the injection. Based on the evidence that α-syn-PFFs cause loss of LTP at 6, 8, and 12 weeks after the injection [18,21], we explored if the synaptic transmission of SPNs of the STR-DL was perturbed as early as 4 weeks after the surgery. The analysis of *ex vivo* electrophysiological recordings shows a typical induction and maintenance of LTP after the application of a high frequency stimulation (HFS) protocol in the STR-DL (Fig. 4A; Paired t test, PBS: pre- *versus* 20 min post-HFS, n = 7, t = 12.06, df = 13, ***P < 0.001 and PFF: pre- *versus* 20 min post-HFS, n = 8, t = 11.25, df = 15, ***P < 0.001). Moreover, the analysis of spontaneous excitatory post-synaptic currents (sEPSCs) in STR-DL SPNs of α-syn-PFFs animals, at this time point, did not reveal glutamatergic transmission differences compared to the PBS group (Fig. 4B; Mann-Whitney's t test; PBS n = 8 *versus* PFF n = 8, frequency: U = 16, amplitude: U = 19, P > 0.05). Thus, these electrophysiological findings in this motor-related area are in line with the absence of motor deficits at this stage of the disease.

To explore the hypothesis that the observed deficits in social behavior are caused by an altered synaptic function in the NAc, we explored the ability of SPNs to express LTP in NAc-Core, a brain region involved in a variety of essential functions related to reward, motivation, and social behavior regulation [22]. In contrast to STR-DL SPNs, NAc-Core neurons of α-syn-PFFs-injected rats (PFF n = 6 and PBS n = 6) did not express this form of synaptic plasticity in response to HFS (Fig. 4C; Paired t test, PBS: pre- *versus* 20 min post-HFS, n = 7, t = 12.04, df = 13, ***P < 0.001 and PFF: pre- *versus* 20 min post-HFS, n = 9, t = 0.49, df = 17, P > 0.05; Two-way ANOVA: interaction x group, $F_{(29,377)}$ = 10.90; ###P < 0.001). These data show that in our model of early synucleinopathy, synaptic plasticity is disrupted in the NAc-Core but not in the STR-DL. Analysis of spontaneous glutamatergic activity in NAc-Core SPNs exhibited a decrease in the sEPSCs frequency but not in the amplitude, suggesting that in this region the loss of LTP might be linked to a reduced release of glutamate from presynaptic terminals (Fig. 4D; Mann-Whitney's t test; PBS n = 8 *versus* PFF n = 8, frequency: U = 0, ***P < 0.001; amplitude: U = 21, P > 0.05).

As the sEPSCs frequency could be associated with a defect in glutamate release, we investigated the protein levels of the two vesicular glutamate transporters 1 and 2 (VGluT1 and VGluT2), which mediate the uptake and sequestration of glutamate in presynaptic vesicles. By confocal analysis, we detected a statistically significant decrease in the VGluT1 puncta density in the NAc-Core in

ARTICLE IN PRESS

the PFF group compared to the PBS, but not in the VGluT2 (Fig. 4E and 4F; Unpaired t-test; PBS n = 5 *versus* PFF n = 5, VGluT1: ***P < 0.001; VGluT2: P > 0.05). These observations suggest that the changes observed in the PFF group result from reduced glutamate release from presynaptic terminals.

Structural plasticity changes are present in the NAc-Core SPNs of α-syn-PFF-injected animals

To explore the possibility that loss of LTP in SPNs recorded in the NAc-Core was also associated with an alteration of structural plasticity, we performed unbiased measurements of spine density (spines/μm), and we evaluated the percentage of each predominant spine following α-syn-PFFs (n = 5) and PBS injections (n = 5). Golgi-staining revealed that α-syn-PFFs affect SPNs spine density in the NAc-Core (Fig. 5B; Mann-Whitney's t-test, PBS *versus* PFF, n = 50, U = 710, ***P < 0.001). Since alterations in the size and shape of synaptic spines are associated with synapse maturation and stability, we analyzed the morphology of spine heads on SPNs across the different experimental groups. Our structural analysis revealed a significant α-syn-PFFs effect on spine density. Specifically, we found a lower density of spines/μm coupled to a lower immature/mature spines ratio in PFF with respect to PBS (Fig. 5C; Mann-Whitney's t-test, PBS *versus* PFF, U = 731, ***P < 0.001). Interestingly, while the PBS group showed notable differences between the overall percentages of immature and mature spines, the PFF group did not exhibit such differences, presenting a comparable number of mature and immature spines (Fig. 5D, PBS group: Immature spines *versus* Mature spines, n = 50, W= -932, ***P < 0.001; PFF group: Immature spines *versus* Mature spines, n = 50, W= -76, P > 0.05).

Further analysis showed that α-syn-PFFs have specific effects on SPNs NAc-Core spine subtypes (Supplementary Fig. 2A). No significant changes were observed in the percentages of thin spines (Supplementary Fig. 2B; Mann-Whitney U test, PBS *versus* PFF: U = 1203, P > 0.05). However, among groups, slight reductions were observed in the percentages of stubby (Supplementary Fig. 2C; Mann-Whitney U test, PBS *versus* PFF: U = 940.5, *P < 0.05) and mushroom spines (Supplementary Fig. 2C; Mann-Whitney U test, PBS *versus* PFF: U = 958.5, *P < 0.05). More interestingly, the PFF group showed a considerable decrease in the percentage of filopodial spines

compared to the PBS group (Supplementary Fig. 2B; Mann-Whitney U test, PBS *versus* PFF: U = 601.5, ***P < 0.001). These findings support our working hypothesis that α-syn-PFFs injection primarily induces structural changes in immature spine populations.

Given these structural dendritic spine changes, we decided to analyze the expression of the post-synaptic density protein 95 (PSD-95), which controls glutamate receptors localization at the synapse [23] and also plays a crucial role in determining spine size and morphology [24]. By confocal analysis, we detected a statistically significant decrease in the PSD-95 puncta density in the NAc-Core in the PFF group with respect to the PBS (Fig. 5E; Unpaired t test; PBS n = 5 *versus* PFF n = 5, PSD-95: *P < 0.05), strengthening the effects of α-syn-PFFs injection on synaptic plasticity.

Differential involvement of DAR and NMDAR in the induction of physiological LTP in STR-DL and NAc-Core regions

Then we employed a pharmacological approach to examine the effects of D1 and D2 DA receptors (DARs, D1R and D2R) subtypes and N-methyl-D-aspartate receptor (NMDAR) subunit (GluN2A and GluN2B) antagonists. Since in STR-DL D1R and GluN2A-NMDAR activation typically mediate LTP under physiological conditions (PBS n = 10), we applied 10 μM of SCH-23390, a D1R antagonist, and 50 nM of NVP, a GluN2A antagonist, before the HFS protocol. The results indicated that these blockers effectively abolished this form of synaptic plasticity (Fig. 6A; Two-way ANOVA: interaction x group, $F_{(1.6,9.5)} = 39$; Control *versus* PBS + NVP 50 nM, n = 6 $^{§§§}P < 0.001$ and Control *versus* PBS + SCH-23390 10 μM, n = 6, $^{§§§}P < 0.001$), supporting the crucial role of these receptors in LTP induction. In contrast, the D2R, sulpiride (5 μM), and GluN2B (ifenprodil 3 μM) antagonists did not produce any effect (Fig. 6A; PBS + ifenprodil 3 μM: Paired t-test pre- *versus* 20 min post-HFS, n = 6, t = 6.67, df = 11, ***P < 0.001; PBS + sulpiride 5 μM: Paired t-test pre- *versus* 20 min post-HFS, n = 6, t = 10.10, df = 11, ***P < 0.001), as previously reported [25,26].

We then performed a novel characterization of the NMDAR subunits and DARs in the NAc-Core region. These receptors may be involved in the induction and maintenance of physiological LTP in SPNs of control animals (PBS n = 14). Our data show that bath application of selective GluN2A antagonist lead to a partial suppression of LTP (about 20 %) (Fig. 6B; left: PBS + NVP 50 nM:

paired t-test pre- *versus* 20 min post-HFS, n = 6, t = 7.156, df = 11, ***P < 0.001); differently in presence of GluN2B antagonist this synaptic plasticity was totally blocked (Fig. 6B; left: Two-way ANOVA: interaction x group, $F_{(1.7,10.4)} = 46$; Control *versus* PBS + NVP 50 nM $^{§§§}P < 0.001$ and Control *versus* PBS + ifenprodil 3 µM, n = 6,$^{###}P < 0.001$).

Interestingly, bath application of both DARs blockers prevented the induction of LTP in SPNs of control rats (Fig. 6B; right: PBS + SCH-23390 10 µM: Paired t-test pre- *versus* 20 min post-HFS, n = 6, t = 3.10, df = 11, *P < 0.05; Two-way ANOVA: interaction x group, $F_{(2.8,16.7)} = 26.90$; Control *versus* PBS + SCH-23390 10 µM, $^{§§§}P < 0.001$ and Control *versus* PBS + sulpiride 5 µM, n = 6, $^{###}P < 0.001$).

Sub-chronic L-Dopa treatment in α-syn-PFFs-injected rats restores LTP in the SPNs of the NAc-Core as well as normal SC

To mitigate the electrophysiological and behavioral changes that were observed in the PFF groups, we administered sub-chronically 10 mg/kg L-Dopa i.p. injection for 3 days.

Following this treatment, animals were tested in the behavioral tasks and sacrificed to perform electrophysiological recordings of SPNs in the NAc-Core region. To test general motivation state in these animals, a sucrose preference test was performed. No significant differences were observed between PBS + L-Dopa (n = 6) and PFF + L-Dopa (n = 6) in both days, displaying a clear preference for sucrose over water (Fig. 7A, One way ANOVA; PBS + L-Dopa *versus* PFF + L-Dopa, Day 1: $F_{(3,20)} = 1.29$, Bonferroni's post hoc test, t = 1.20, df = 20, P > 0.05; Day 2: $F_{(3,20)} = 2.42$, Bonferroni's post hoc test, t = 2.02, df = 20, P > 0.05).

To evaluate the effect of L-Dopa treatment in the social deficits observed in PFF animals, we performed a free-social interaction and a three-chamber tests.

We found that at 4 weeks post-surgery, PFF rats (n = 6) subjected to L-Dopa treatment explored the inanimate object similarly to the untreated rats (Fig. 7B; left graph, One way ANOVA, $F_{(3,19)} = 4.06$, P = 0.02; Mann-Whitney's t-test, object: PFF *versus* PFF + L-Dopa, U = 5, P > 0.05). Conversely, the interest in approaching the conspecific rats (Fig. 7B; right graph, One way ANOVA, $F_{(3,19)} = 20.51$, P = 0.00001; Mann-Whitney's t-test; social: PFF *versus* PFF + L-Dopa, U = 2, *P < 0.05) was restored after 3 days of L-Dopa treatment. As expected, L-Dopa administration in PBS animals (n = 6) preserved the sociability as in control rats (Fig. 7B; right

graph, One way ANOVA, $F_{(3,19)} = 20.51$, P = 0.00001; Mann-Whitney's t-test; object: PBS *versus* PBS + L-Dopa, U = 4, P > 0.05, social: PBS *versus* PBS + L-Dopa, U = 10, P > 0.05). Then, sociability and social novelty preferences were also assessed using the three-chamber task. The marked social deficits observed in PFF animals (Fig. 3C) were significantly restored, with a preference for ST and NT respect to E and FT, correspondingly (Fig. 7C, left; One way ANOVA, $F_{(3,20)} = 18.20$, Bonferroni's post hoc test, t = 3.12, df = 20, PFF + L-Dopa: ST *versus* E, *P < 0.05; right; One way ANOVA, $F_{(3,20)} = 10.93$, Bonferroni's post hoc test, t = 3.58, df = 20, PFF + L-Dopa: NT *versus* FT, *P < 0.05). Specifically, both in sociability and social novelty sessions, PFF + L-Dopa animals approached significantly more to ST and NT respect the inner control group (PFF), resembling the behaviour of PBS + L-Dopa rats (Fig. 7C, left; One way ANOVA, $F_{(8,40)} = 19.14$, Bonferroni's post hoc test, t = 4.56, df = 40, PFF *versus* PFF + L-Dopa: **P < 0.01 and t = 1.96, df = 40, PBS + L-Dopa *versus* PFF + L-Dopa: *ns*, P > 0.05; right; One way ANOVA, $F_{(8,40)} = 8.79$ Bonferroni's post hoc test, t = 6.89, df = 40, PFF *versus* PFF + L-Dopa: ***P < 0.001, and t = 0.93, df = 40, PBS + L-Dopa *versus* PFF + L-Dopa: *ns*, P > 0.05). As expected, L-Dopa treatment did not perturb social behavior in PBS animals (Fig. 7C, left; One way ANOVA, $F_{(8,40)} = 19.14$, Bonferroni's post hoc test, t = 7.88, df = 40, PBS + L-Dopa: ST versus E, ***P < 0.0001; right; One way ANOVA, $F_{(8,40)} = 8.79$ Bonferroni's post hoc test, t = 5.58, df = 40, PBS + L-Dopa: NT *versus* FT, *P < 0.05).

Overall, these results suggests that sub-chronic L-Dopa treatment effectively normalized the social impairments caused by α-syn-PFFs 4 weeks after injection. Remarkably, L-Dopa treatment also fully restored LTP induction in NAc-Core SPNs (Fig. 6D; Paired t test, PFF + L-Dopa: pre- *versus* 20 min post-HFS, n = 9, t = 10.90, df = 17, ***P < 0.001; Two-way ANOVA: interaction x group, F(29,464) = 13.94; PFF *versus* PFF + L-Dopa, $^{###}$P < 0.001).

ARTICLE IN PRESS

ARTICLE IN PRESS

Discussion

SC represents a psychological process that enables a subject to understand how other people intend to act, feel, and think [27]. The ability to learn from the experiences of other subjects is essential for survival. The social environment allows us to learn and maintain critical skills, such as walking, communicating, and avoiding dangerous situations. Even in small mammals, social interaction, and memory processes guide food preference, exploration of novel contexts, and social approach [28]. Accordingly, when a rodent has social interactions with a novel conspecific, ensembles of cells embedded across neural circuits are activated to form a stable representation of social memories within a neuronal circuit, including the hippocampus, the amygdala, and the NAc [28].

Although impairments in social communication are also a hallmark of several neurological and psychiatric disorders, little is known about the mechanisms underlying these abnormalities. Dopaminergic pathways are possible candidate neurotransmitter systems in mediating SC. For this reason, in PD research, great attention has recently been paid to investigating the mechanisms and consequences of dysfunctional SC. Interestingly, SC impairment affects about one-third of PD patients in the early stages of the disease and is the most common neuropsychological deficit in this precocious phase [7].

At this point, however, we raised a simple but important question: can a deficit in SC occur in a premotor stage of PD? To address this crucial question, we used a model of early synaptopathy induced by striatal α-syn PFFs injection. Our previous study[18] demonstrated loss of synaptic plasticity in SPNs of the dorsolateral striatum, and alterations in motor performances as early as 6 weeks post-injection of α-syn PFFs. Thus, we can assume that this 6-week time window represents a phase of the neurodegenerative process in which an early motor phase dysfunction becomes detectable in the experimental disease model. In the present study, we aimed to investigate an even earlier time point (4 weeks post-injection) to potentially capture a phase in which motor deficits are not yet evident, but subclinical behavioral changes may already be measurable. In this model, we analyzed the integrity of the nigrostriatal dopaminergic terminals at the earliest time point ever explored, 4 weeks after lesioning. In the STR-DL, TH^+ and DAT immunostaining intensity showed no difference compared to control PBS-injected rats, suggesting the integrity of dopaminergic presynaptic terminals in this motor-related region. On the contrary, our data show that these two markers were reduced in NAc-Core, suggesting that, in this model, the dopaminergic innervation

ARTICLE IN PRESS

is selectively affected in this limbic area. Interestingly, brain sections from the PBS and PFF groups showed that the number of TH+ neurons was not altered in either the SNpc or the VTA, suggesting that the observed early degeneration of the dopaminergic system is specific for the neuronal terminals and does not affect the somatic region of the DA neurons.

Notably, the immunostaining intensity of the pathological form of α-syn, p129-αSyn, was more pronounced in the NAc-Core than in the STR-DL. At the same time, no differences were observed in the SNpc *versus* the STR-DL, again suggesting that the pathological mechanism in this early stage is more pronounced in the axonal terminal region rather than in the somatic area.

To demonstrate that our rodent model represents a premotor stage of the disease, we measured motor functions and found no change in motor learning and coordination skills. In our experiments, both α-syn-PFFs- and PBS-injected animals similarly learned the tasks, demonstrating that our model reflects a premotor stage of the disease.

Since deficits in social interaction have been reported in PD patients at early stages, we explored this cognitive domain in our premotor model of synucleinopathy. First, we assessed whether, under our experimental conditions, α-syn-PFF injection at this time point leads to alterations in reward-related behavior. The consistent results obtained from the sucrose preference test across all groups indicate that motivational processes remain intact and there is no evidence of anhedonia.

To evaluate social deficits, we examined the social interaction behavior of α-syn-PFF–injected rats when exposed to a conspecific in the test cage. We observed a reduced ability of α-syn-PFF rats to engage in social interaction compared to controls. In contrast, no differences were found between the PFF and PBS groups in the time spent exploring an inanimate object, suggesting that general exploratory behavior was unaffected. Furthermore, rats were tested in the three-chamber paradigm, a well-established task for assessing social behaviors, including sociability and preference for social novelty. Our results revealed a reduced preference for the social target during the sociability phase and for the novel social target during the social novelty session, indicating an impairment in the SC domain.

Interestingly, however, in the object recognition test, α-syn-PFFs-injected rats, in contrast with PBS group, explored in the same manner both the displaced and the non-displaced objects. The specific lack of interest in the object position in the arena suggests a deficit in spatial discrimination in the α-syn-PFF-injected group. These findings are consistent with the literature showing that patients at the early stages of PD have difficulties in interpreting social signals and maintaining

interpersonal relationships, in addition to a deficit in visuo-spatial functions [7]. They also support the hypothesis that SC impairment occurs in a premotor stage of this model of synucleopathy.

A further step in our investigation was to test the hypothesis that the observed deficits in social behavior are caused by an altered synaptic function in SPNs of the NAc-Core, a key structure implicated in the complex non-motor functions regulated by DA [22]. Consistent with our hypothesis, we found that the ability of NAc-Core SPNs to express LTP was lost in α-syn-PFF-injected animals. In contrast, STR-DL SPNs expressed physiological synaptic plasticity in response to the HFS protocol in the same experimental condition. In addition, we observed a reduction in the frequency of spontaneous glutamatergic activity in SPNs of the NAc-Core, in the absence of changes in its amplitude. This condition could potentially contribute to the loss of LTP in the NAc-Core, since glutamate is essential for the activation of NMDA receptors, which, in turn, is necessary for the induction of LTP [29]. It is known that sEPSC frequency generally reflects presynaptic effects, mainly related to glutamate release, which is finely regulated by VGluTs, which are responsible for packaging glutamate into synaptic vesicles [30,31]. VGluTs levelst that are critical for the balance between excitation and inhibition [32] and synaptic transmission [30,33], are altered in several pathological conditions such as Alzheimer's disease [34], PD [35–37] and Amyotrophic Lateral Sclerosis [38]. In this study, we showed that VGluT1 puncta were significantly reduced in the NAc-Core of PFF animals, whereas VGluT2 levels were unaffected. Since VGluTs control the amount and also the probability of glutamate release [30,31], the reduced VGluT1 puncta are therefore consistent with the lower frequency of sEPSCs in SPNs of the NAc-Core of PFF animals, although a reduced vesicular turnover cannot be excluded.

The NAc receives glutamatergic afferents from the basolateral amygdala [39], the ventral hippocampus [40], the prefrontal cortex (PFC) [41] and the paraventricular nucleus of the thalamus (PVT) [42]. VGluT1 puncta mainly represent the input from the PFC, whereas VGluT2 puncta mainly represent the input from the PVT [30,43–45]. In our PFF-injected animals, we observed a selective reduction in VGluT1 puncta within the NAc, with no significant change in VGluT2. This finding suggests a preferential disruption of cortical afferents, especially those originating from the PFC. Such selective vulnerability aligns with growing evidence of input-specific susceptibility to α-syn pathology. Our results are consistent with recent findings by Bellingacci and colleagues [46], which reported greater degeneration in corticostriatal than in thalamostriatal pathways in a

ARTICLE IN PRESS

model of α-syn oligomer-induced synucleinopathy. The reduction in VGluT1 signal supports the notion of functional disconnection within the PFC–NAc circuitry, which may contribute to early synaptic dysfunction and behavioral deficits in α-synucleinopathies.

In the NAc-Core, the majority of extrinsic glutamatergic inputs reach the distal dendrites and spines of the SPNs, whereas the local inputs contact the proximal dendrites and spines. Given this arrangement, we investigated whether the loss of LTP in SPNs recorded in the NAc-Core could be associated with altered structural plasticity of the distal spines targeted by the glutamatergic inputs. Interestingly, unbiased analyses revealed a lower density of dendritic spines/μm coupled with a lower ratio of immature-to-mature spines in the PFF compared to the PBS group. This is in accordance with the work of Wu and colleagues, showing that α-syn fibrils dramatically affect the density of dendritic spines [47]. Since the vast majority of spines typically contain an excitatory synapse [48], we hypothesized that the reduced spine density following α-syn-PFFs injection could explain the reduced excitatory synapse density observed in our model. This finding is consistent with the notion that the number of spines, and hence the number of synapses, is directly related to the frequency of sEPSCs.

In addition to a reduced number of dendritic spines/μm in the SPNs of the NAc-Core, which was associated with a reduced density of VGluT1 puncta, PFF animals showed a reduced density of PSD-95 puncta. PSD-95 is one of the most abundant proteins in the postsynaptic density of excitatory synapses. It controls glutamate receptor localization at the synaptic cleft [23] and also plays a crucial role in determining spine size and morphology [24]. A previous study has shown that overexpression of PSD-95 in developing neurons can cause an increase in EPSC frequency but not EPSC amplitude [49], suggesting that a lower level of PSD-95 can significantly influence EPSC frequency as well as spine morphology. Previous studies have shown that the formation of α-syn aggregates reduces synaptic protein levels, including synaptic vesicle-associated SNARE proteins, and progressively disrupts neuronal network activity [50].

The discrepancy between the complete loss of LTP in the NAc and the partial reduction in spine density indicates that the remaining excitatory synapses, including those originating from thalamic (VGlut2-positive) inputs, are insufficient to support synaptic plasticity. One possible explanation is that corticostriatal (VGlut1-positive) synapses[45], which appear selectively impaired, play a predominant role in the induction of LTP under the stimulation protocols used. Moreover, the loss of immature spines—typically more plastic and responsive to activity—may disproportionately

affect the capacity for LTP, despite the preservation of some mature spines and thalamic terminals. Alternatively, α-syn pathology may induce broader functional impairments at the synaptic level, such as altered receptor function, disrupted signaling pathways, or impaired integration of synaptic input, which collectively prevent LTP even at structurally intact synapses. These findings underscore the complexity of synaptic dysfunction in PFF models and point to the need for input-specific and functional analyses to disentangle structural from physiological effects.

Taken together, our results suggest that alteration of glutamatergic input to the SPNs of the NAc-Core may be one of the first consequences of the formation of fibrillary α-syn and that these synaptic changes may contribute to the observed neuronal dysfunction and behavioral abnormalities.

The final step of our investigation was to explore the possibility of restoring dysfunctional synaptic plasticity and SC by a pharmacological approach. To address this issue, we have characterized the features of physiological LTP in the SPNs of NAc-Core. In these neurons, LTP requires, differently from what is observed in STR-DL SPNs, not only GluN2A-expressing NMDAR but also activation of GluN2B-expressing receptors. The GluN2B subunit might be particularly important in enabling a synapse to undergo bidirectional changes. Moreover, the presence of GluN2B subunit-containing NMDA receptors may be a prerequisite for facilitating the potentiation of the synapses, allowing the interaction of this NMDA subunit with calcium/calmodulin-dependent protein kinase II, a molecular step that is crucial for long-lasting plasticity [51]. Concerning the dopaminergic regulation of LTP in the SPNs of NAc-Core, again in sharp contrast to what was observed in the STR-DL, we observed that not only D1R but also D2R play a critical role. This pharmacological feature could be explained by either the co-expression of these two DARs on the same neuron or by a network modulatory effect involving multiple neuronal subtypes within this structure. The critical role of DA in the plastic changes of the SPNs of NAc-Core may also account for the modulation of reward, arousal, and motivational responses, and studies report that DA level changes in NAc during social behaviors [22,52,53]. Thus, we hypothesized that in our experimental model of premotor PD, an increase of endogenous DA would also lead to a recovery of synaptic plasticity, as well as to a normalization of SC. Our hypothesis was confirmed by a key experiment showing that sub-chronic L-Dopa, a precursor of DA, was able to restore both LTP and normal social behavior.

ARTICLE IN PRESS

In recent years, several studies have shown that DA modulates social learning [54,55] through striatal DAR signaling [56]. These observations suggest that dysfunction within DA pathways may affect SC in movement disorders [57]. These findings also seem to suggest that, at least in the early stage of PD natural history, treatment with low doses of L-Dopa may restore social learning. This mild phase of the disease is associated with a low degree of DA denervation, a condition that is mimicked by our α-syn-related model. In this context, sub-chronic L-Dopa treatment was able to restore physiological synaptic plasticity within the NAc and to rescue deficits in social behavior. Indeed, administration of this dopaminergic agonist led to a clear improvement in both sociability and preference for social novelty, as evidenced in the free-social interaction and three-chamber tests. These findings suggest that dopaminergic signaling plays a crucial role in modulating social behavior during the early, prodromal stages of synucleinopathy. Conversely, in the advanced phase of the disease, the full dopaminergic denervation causes abnormal motor responses to L-Dopa, such as dyskinesia and motor fluctuations, as well as impulse control disorders. This severe condition is not mimicked by the mild model utilized in the present study, but can be observed after a full denervation induced by 6-OHDA injection [58]. In this framework, dopaminergic therapy re-establishes tonic DA levels, allowing the motivation to act socially. These findings also strengthen the idea that social interaction engagement and reward processing share common anatomical substrates. Sectors of the basal ganglia, in a cooperative manner with the NAc, encode reward components and are involved in motivating interactions in social contexts. In conclusion, our hypothesis is that in both physiological conditions as well as in the early PD pathological state, SC is respectively orchestrated by endogenous DA and L-Dopa treatment.

In the present study, we have shown that a form of synucleinopathy, at its earlier phases, before the appearance of subtle motor symptoms associated with dorsolateral striatum synaptic alterations, is a good model of PD at a premotor stage. Since in our study seeding of α-syn pathology is present in brain regions interconnected with the injected site (in particular in the cortex), one might postulate that this model mimics Lewy Body Dementia rather than PD. Although this doubt can be raised, a critical point makes it unlikely. Several clinical studies found that in Lewy Body Dementia, the L-Dopa treatment causes a worsening of the behavioral deficits [69,70], while in PD patients, early treatment with this drug induces clinical amelioration. In line with this latter evidence, we found that sub-chronic treatment with L-Dopa restores the SC and synaptic plasticity in the NAc. Thus, we believe that considering our model as a pre-motor PD can be

ARTICLE IN PRESS

ARTICLE IN PRESS

reasonable. In this condition, mild dopaminergic denervation in the NAc-Core is sufficient to induce SC deficit and changes in synaptic plasticity. Our results provide a novel mechanistic view in which an impairment of VTA-NAc dopaminergic projection causes deficits in SC and, in line with this idea, an increase of endogenous DA restored both synaptic and behavioral alterations. Moreover, the behavioral changes associated with the functional alterations observed suggest that the NAc plays a fundamental role in the premotor phase of PD and should therefore be taken into account in the early diagnosis and treatment of this neurodegenerative disease.

Methods

Animals

Male Wistar rats of two to three months (300-350 g) (n = 114, 66 PBS- and 48 PFF- injected animals) were group-housed with *ad libitum* access to food and water during a 12 h light/dark cycle. All efforts were made to reduce the number of rats used and their suffering in accordance with the European Directive (2010/63/EU). All procedures performed were conducted in accordance with national animal standards, following the guidelines of animal science associations (FELASA), and were approved by the Italian Ministry of Health. Rats were injected with α-syn-PFFs or PBS. Four weeks after the injection, rats were subjected to behavioral tests and then sacrificed for electrophysiological recordings and tissue analysis (Fig. 1A). Specifically, 59 animals were used for behavioral testing and morphological analysis, while 55 rats were used for electrophysiological assessment.

ARTICLE IN PRESS

A-syn Preformed Fibrils (PFFs) Preparation and Stereotaxic Injection

PFFs were prepared from lyophilized fresh human monomeric α-syn (0.33 mg) as already reported [19]. In detail, fibril formation was induced by incubating the protein under constant agitation (600 rpm) at 37°C in benchtop tubes. The samples were placed on an orbital shaker (Eppendorf Thermomixer) for 7 days, and the aggregation process was monitored using the thioflavin T (ThT) fluorescence assay. Prior to injection, α-syn-PFF aliquots were sonicated in an ultrasonic bath for a total of 60 pulses (0.5 s each, totaling 30 s). Animals were deeply anesthetized with a mix of Zoletil (an anesthetic drug; 50/50 mg/ml tiletamine and zolazepam) and Rompun (sedative drug;

ARTICLE IN PRESS

20 mg/ml xylazine hydrochloride) and were bilaterally injected with 1 µl of PBS (vehicle) or human-α-syn-PFFs into the STR-DM, as previously described [21]. Stereotaxic striatal injections coordinates, taken with a tooth bar set at 0.00, were: (i) anteroposterior (AP) +1.0, mediolateral (ML) +3.0, dorsoventral (DV) −5.0; and (ii) AP +1.0, ML −3.0, DV −5.0.

L-Dopa administration

Rats (n = 12 PFF and n = 6 PBS) were administered with L-Dopa (10 mg/kg) and benserazide (6 mg/kg) once a day for 3 consecutive days (sub-chronic intraperitoneal, i.p. treatment) 4 weeks post-injection. These animals were then subjected to behavioral assessments and electrophysiological recordings.

Behavioral tests

Open field task: The animals were tested for 10 min (600 s) in an empty open field arena (60 cm X 60 cm) to evaluate their locomotion and exploratory activity. Using the open field test, it is also possible to observe anxiety-like behaviors by evaluating the amount of time spent in the peripheral sectors, as the center of the arena is generally anxiogenic for rodents[59].

Visuo-spatial memory task: A modified version of the object recognition test was used as a visuo-spatial memory task to detect impairment in spatial-related processes in different animal models of PD. Rats, placed into an empty open field arena (60 cm X 60 cm), were individually submitted to consecutive 6-min sessions, as previously described [60–62].

Inclined grid walking task: We tested the motor coordination of rats injected with α-syn-PFFs compared with control animals. Animals were forced to walk on a grid divided into 16 quadrants (4 quadrants x 4 rows), inclined at 45° and 112 cm x 60 cm in size [21]. The animal was placed at the bottom of the grid and was allowed to reach the top of the grid for a maximum of 5 min (300s)[18].

Rotarod test: The accelerating Rotarod was used to assess motor coordination and balance. The apparatus (Ugo Basile) consists of a rod (6 cm in diameter) suspended horizontally at a height of 14 cm above the floor. To begin, rats were habituated to the rotating rod set at low speed for at least 60 s. During the test, the rotation speed of the rod was accelerated from 4 rpm to 40 rpm in 300 s, and the latency of falling from the rod was measured with a time limit of 600 s [63].

ARTICLE IN PRESS

Free social interaction test: A free social interaction test was employed for the behavioral assessment of the interactions with a conspecific[64]. During the test, each animal was placed in an arena for a maximum of 5 min (300 s). Each rat was exposed to both an inanimate object and a novel conspecific (another animal of the same species). The animal's behaviors, such as sniffing and other social interactions, were recorded and analyzed [65].

Sucrose preference test: This test evaluates sensitivity to natural rewards by measuring an animal's preference for a 1% sucrose solution over water. Animals were singly housed and habituated to drinking from two identical bottles. During the 72-hour test, both bottles were available, with sucrose and water positions alternated daily to prevent side bias. Bottles were refilled daily and intake was measured using graduated cylinders. Preference intake was expressed as the percentage of sucrose and water intake over total fluid consumed [66].

Three-chamber test: We tested the sociability and social novelty preference using a rectangular Plexiglas box divided into three equal chambers (one central and two lateral). Clear partitions with small openings allow free movement between chambers. The social, familiar, or novel animals were placed inside the perforated wire cages to allow sniffing but limit aggressive or sexual interaction between animals. The test is characterized by three sessions of 10 min: (I) The first session was habituation in which the subject mouse adapted to the empty three chambers (data not shown); (II) the second session was "sociability" in which the subject rat encountered a social target, ST (never-before-met) in a wired cage over one lateral chamber and an empty wired cage over the opposite lateral chamber; (III) the third session was "social novelty" in which the wire cage enclosing the familiar rat (FT) (the social target in the sociability session), and a second novel animal (novel target, NT) (never-before-met) was placed in the other lateral chamber in a wired cage (Fig. 3C and 7C) [67]. Data analysis were made by Smart 3.0 software (Harvard Apparatus, PanLab) and the % sniffing-facing time over the entire time (600 s) was plotted.

Immunofluorescence and confocal analysis

After behavioral tests, animals were deeply anesthetized by intraperitoneal (i.p.) injections of Rompun and Zoletil. As previously described, to model α-syn pathology, a single dose of PFFs was injected into the striatum. To assess the propagation of α-syn aggregates, we analyzed the fluorescent presence of phosphorylated α-syn, as an index of PFFs, in predetermined and random

ARTICLE IN PRESS

regions of interest (ROIs) across various brain areas. The extent of spreading was quantified by measuring the signal's optical density (O.D.). All the immunohistochemical and immunofluorescence staining followed identical protocols regarding tissue permeabilization, antibody combinations, and densitometric analysis [21]. Representative images were prepared by adjusting the brightness and contrast of digital images in a consistent manner across all conditions. All quantitative analyses were performed blind to the animal's experimental group assignment.

Immunohistochemistry and stereological analysis of dopaminergic neurons in SNpc and VTA

To evaluate the impact of the intrastriatal injections of PFFs in SNpc and VTA, stereological cell counts of TH^+ neurons were conducted. The stereological analysis was carried out on brain sections presenting the SNpc and the VTA regions. To cover the rostro-caudal extension of the analyzed regions, 10 sections were counted for each animal. For TH immunohistochemistry, primary and secondary antibodies and ABC-HRP solutions were prepared as previously reported [21,68].

ARTICLE IN PRESS

Golgi staining

After perfusion, the brains were dissected and divided into two hemispheres. After sampling, brains were rapidly rinsed in Milli-Q water and then impregnated according to the FD Rapid GolgiStain™ Kit manufacturer's instructions (FD NeuroTechnologies, Inc.). Completed Golgi-Cox staining, 150 µm of coronal slices were obtained through a cryostat. Dendritic spines density, filopodia, thin, mushroom, and stubby spines were analyzed using Neurolucida® software (MBF Bioscience) and then calculated from pooled values (10 dendrites *per* animal). Images were obtained with a 100x immersion oil objective using an optical microscope.

Electrophysiological experiments

Animals were sacrificed to obtain corticostriatal slices for electrophysiological recordings. Brain slices were cut for intracellular (thickness 280 µm) and whole-cell patch clamp recording

ARTICLE IN PRESS

(thickness 240 μm) using a vibratome[69], and transferred to a recording chamber, with a continuously flowing Krebs solution (RT; rate 2.5–3 ml/min) [21].

For whole-cell patch clamp, recordings of the SPNs (voltage clamped at −70 mV) were performed with borosilicate glass pipettes (5-8 MΩ) filled with the internal solutions [19,21]. Whole-cell access resistance (15–35 MΩ) was monitored throughout the experiments, and variations of this parameter higher than 20% led to the rejection of the experiment. For intracellular recordings, sharp electrodes were filled with 2 M KCl (30–60 MΩ).

For STR-DL recordings, the stimulation electrodes were placed inside the corpus callosum. For NAc experiments, the recording electrodes were placed in the NAc-Core. Spontaneous excitatory postsynaptic potentials (EPSPs) were evoked by electrical stimulation, and to induce the LTP, we applied an HFS protocol[69].

Contrary to STR-DL, induction of the LTP protocol in NAc-Core does not require the removal of magnesium ions from the recording solution because NMDAR is always present in an active state [70]. All the experiments were performed in the continuous presence of Picrotoxin (50 μM).

The pharmacological study of LTP was performed with 10-min bath application of D1R, D2R, GluN2A and GluN2B antagonists (SCH-23390 10 μM, sulpiride 5 μM, NVP 50 nM, and ifenprodil 3 μM) before HFS protocol.

ARTICLE IN PRESS

Statistical analysis

Data were analyzed using GraphPad Prism 6.0. Statistical significance was set at $P < 0.05$, $P < 0.01$, and $P < 0.001$ (reported in the Results section and/or Figure legends). Data are expressed as mean ± SEM.

Behavior: motor and cognitive-behavioral data were analyzed using Student's *t*-test, One-way ANOVA and Two-way ANOVA with treatment (PBS *versus* PFF and PBS + L-Dopa *versus* PFF + L-Dopa) as a factor. Bonferroni's post-hoc test was applied when appropriate.

Electrophysiology: changes in synaptic strength were assessed by measuring EPSC and EPSP amplitude, expressed as percentage change from baseline (measured 20 min post-stimulation). Group comparisons were made using two-way ANOVA with Bonferroni's post-hoc test. Student's *t*-test was used to compare pre- (averaged at 2nd and 4th min) *versus* post-HFS (mean of 18th and

ARTICLE IN PRESS

20th min) within the same cell, and to compare EPSC amplitudes under different drug conditions. Electrophysiological data were analyzed offline using Clampfit 10.6 (Molecular Devices).
Morphology and Immunostaining: data were analyzed with Student's *t*-test.

Data availability

Data are provided within the paper or in Supplementary Materials.

Acknowledgements

This work was supported by grants from: the Italian Ministry of Health in the Next Generation EU Program - Piano Nazionale di Ripresa e Resilienza (PNRR) – Mission 6C2 - 2.1 ‘’Valorizzazione e potenziamento della ricerca biomedica del SSN’’- PNRR-MAD-2022-12375804, “Clinical, molecular and electrophysiological profiling of Parkinson's Disease: the role of nonpharmacological therapies” – CUP: F23C22001130007; Italian Ministry of Education, University and Research (MIUR)- Italian Ministry of Health, Ricerca Corrente (P.C.), Italian Ministry of University and Research (MUR), PNRR project MNESYS (PE0000006).

Author contributions

P.C. and G.M. conceived and designed the study. G.M., F.C., G.N. and V.G. designed and performed electrophysiological recordings. P.C. supervised the electrophysiology experiments. M.E.C. took care of the animal ethical and health issues. F.C., G.M., G.N. and F.S. designed, performed, and analyzed the behavioral experiments. M.D.C., F.S., S.N., and M.T.V. designed and carried out the immunohistochemistry, immunofluorescence and DA neuron counting experiments. M.T.V. supervised these experiments. P.C., V.G., G.M. and F.C. wrote the first draft of the manuscript. P.C., V.G. and M.T.V. revised the manuscript. All authors discussed the results and commented on the manuscript.

Competing interests

The authors declare that they have no competing interests

References

1. Poewe W, Seppi K, Tanner CM, et al. Parkinson disease. *Nat Rev Dis Primers*. 2017;3(1):17013. doi:10.1038/nrdp.2017.13
2. Calabresi P, Mechelli A, Natale G, Volpicelli-Daley L, Di Lazzaro G, Ghiglieri V. Alpha-synuclein in Parkinson's disease and other synucleinopathies: from overt neurodegeneration back to early synaptic dysfunction. *Cell Death Dis*. 2023;14(3):176. doi:10.1038/s41419-023-05672-9
3. Calabresi P, Di Lazzaro G, Marino G, Campanelli F, Ghiglieri V. Advances in understanding the function of alpha-synuclein: implications for Parkinson's disease. *Brain*. 2023;146(9):3587-3597. doi:10.1093/brain/awad150
4. Citro S, Lazzaro G Di, Cimmino AT, Giuffrè GM, Marra C, Calabresi P. A multiple hits hypothesis for memory dysfunction in Parkinson disease. *Nat Rev Neurol*. 2024;20(1):50-61. doi:10.1038/s41582-023-00905-z
5. Fernández-Fernández R, Lahera G, Fernández-Rodríguez B, et al. Social Cognition and Mild Cognitive Impairment in Mid-Stage Parkinson's Disease. *Behavioral Sciences*. 2024;14(2):101. doi:10.3390/bs14020101
6. Seebacher F, Krause J. Physiological mechanisms underlying animal social behaviour. *Philosophical Transactions of the Royal Society B: Biological Sciences*. 2017;372(1727):20160231. doi:10.1098/rstb.2016.0231
7. Czernecki V, Benchetrit E, Houot M, et al. Social cognitive impairment in early Parkinson's disease: A novel "mild impairment"? *Parkinsonism Relat Disord*. 2021;85:117-121. doi:10.1016/j.parkreldis.2021.02.023
8. Seubert-Ravelo AN, Yáñez-Téllez MG, Lazo-Barriga ML, Calderón Vallejo A, Martínez-Cortés CE, Hernández-Galván A. Social Cognition in Patients with Early-Onset Parkinson's Disease. *Parkinsons Dis*. 2021;2021:1-13. doi:10.1155/2021/8852087
9. Trompeta C, Gasca-Salas C, Pineda-Pardo JA, et al. Longitudinal assessment of social cognition in de novo Parkinson's disease patients and its relationship with dopaminergic innervation. *Behavioural Brain Research*. 2023;454:114654. doi:10.1016/j.bbr.2023.114654
10. Slomp AC, van der Zee S, Boertien JM, Gerritsen MJJ, van Laar T, Spikman JM. Impaired facial emotion recognition in relation to social behaviours in de novo Parkinson's disease. *J Neuropsychol*. 2024;18(2):205-216. doi:10.1111/jnp.12341
11. Eddy CM. Basal ganglia contributions to social cognition: evidence from movement disorders. *Cogn Neuropsychiatry*. 2025;30(1):1-14. doi:10.1080/13546805.2025.2490054
12. Calabresi P, Picconi B, Tozzi A, Ghiglieri V, Di Filippo M. Direct and indirect pathways of basal ganglia: a critical reappraisal. *Nat Neurosci*. 2014;17(8):1022-1030. doi:10.1038/nn.3743
13. Schuster BA, Sowden S, Rybicki AJ, et al. Disruption of dopamine D2/D3 system function impairs the human ability to understand the mental states of other people. *PLoS Biol*. 2024;22(6):e3002652. doi:10.1371/journal.pbio.3002652
14. Liu Q, Shi J, Lin R, Wen T. Dopamine and dopamine receptor D1 associated with decreased social interaction. *Behavioural Brain Research*. 2017;324:51-57. doi:10.1016/j.bbr.2017.01.045

ARTICLE IN PRESS

15. Smith ML, Asada N, Malenka RC. Anterior cingulate inputs to nucleus accumbens control the social transfer of pain and analgesia. *Science (1979)*. 2021;371(6525):153-159. doi:10.1126/science.abe3040
16. Choi TY, Jeon H, Jeong S, et al. Distinct prefrontal projection activity and transcriptional state conversely orchestrate social competition and hierarchy. *Neuron*. Published online December 2023. doi:10.1016/j.neuron.2023.11.012
17. Terracciano A, Luchetti M, Karakose S, Stephan Y, Sutin AR. Loneliness and Risk of Parkinson Disease. *JAMA Neurol*. 2023;80(11):1138. doi:10.1001/jamaneurol.2023.3382
18. Tozzi A, Sciaccaluga M, Loffredo V, et al. Dopamine-dependent early synaptic and motor dysfunctions induced by α-synuclein in the nigrostriatal circuit. *Brain*. 2021;144(11):3477-3491. doi:10.1093/brain/awab242
19. Durante V, de Iure A, Loffredo V, et al. Alpha-synuclein targets GluN2A NMDA receptor subunit causing striatal synaptic dysfunction and visuospatial memory alteration. *Brain*. 2019;142(5):1365-1385. doi:10.1093/brain/awz065
20. Vandendriessche C, Bruggeman A, Foroozandeh J, et al. The Spreading and Effects of Human Recombinant α-Synuclein Preformed Fibrils in the Cerebrospinal Fluid of Mice. *eNeuro*. 2024;11(3):ENEURO.0024-23.2024. doi:10.1523/ENEURO.0024-23.2024
21. Marino G, Campanelli F, Natale G, et al. Intensive exercise ameliorates motor and cognitive symptoms in experimental Parkinson's disease restoring striatal synaptic plasticity. *Sci Adv*. 2023;9(28). doi:10.1126/sciadv.adh1403
22. Berridge KC, Robinson TE. What is the role of dopamine in reward: hedonic impact, reward learning, or incentive salience? *Brain Res Rev*. 1998;28(3):309-369. doi:10.1016/S0165-0173(98)00019-8
23. Cały A, Śliwińska MA, Ziółkowska M, et al. PSD-95 in CA1 Area Regulates Spatial Choice Depending on Age. *The Journal of Neuroscience*. 2021;41(11):2329-2343. doi:10.1523/JNEUROSCI.1996-20.2020
24. El-Husseini AE, Schnell E, Chetkovich DM, Nicoll RA, Bredt DS. PSD-95 involvement in maturation of excitatory synapses. *Science*. 2000;290(5495):1364-1368.
25. Centonze D, Picconi B, Gubellini P, Bernardi G, Calabresi P. Dopaminergic control of synaptic plasticity in the dorsal striatum. *European Journal of Neuroscience*. 2001;13(6):1071-1077. doi:10.1046/j.0953-816x.2001.01485.x
26. Natale G, Pignataro A, Marino G, et al. Transcranial Magnetic Stimulation Exerts "Rejuvenation" Effects on Corticostriatal Synapses after Partial Dopamine Depletion. *Movement Disorders*. 2021;36(10):2254-2263. doi:10.1002/mds.28671
27. Adolphs R. The Social Brain: Neural Basis of Social Knowledge. *Annu Rev Psychol*. 2009;60(1):693-716. doi:10.1146/annurev.psych.60.110707.163514
28. Leblanc H, Ramirez S. Linking Social Cognition to Learning and Memory. *The Journal of Neuroscience*. 2020;40(46):8782-8798. doi:10.1523/JNEUROSCI.1280-20.2020
29. Turner BD, Kashima DT, Manz KM, Grueter CA, Grueter BA. Synaptic Plasticity in the Nucleus Accumbens: Lessons Learned from Experience. *ACS Chem Neurosci*. 2018;9(9):2114-2126. doi:10.1021/acschemneuro.7b00420
30. Fremeau RT, Voglmaier S, Seal RP, Edwards RH. VGLUTs define subsets of excitatory neurons and suggest novel roles for glutamate. *Trends Neurosci*. 2004;27(2):98-103. doi:10.1016/j.tins.2003.11.005
31. Takamori S. VGLUTs: 'Exciting' times for glutamatergic research? *Neurosci Res*. 2006;55(4):343-351. doi:10.1016/j.neures.2006.04.016

ARTICLE IN PRESS

32. Seal RP, Akil O, Yi E, et al. Sensorineural Deafness and Seizures in Mice Lacking Vesicular Glutamate Transporter 3. *Neuron*. 2008;57(2):263-275. doi:10.1016/j.neuron.2007.11.032
33. Wojcik SM, Rhee JS, Herzog E, et al. An essential role for vesicular glutamate transporter 1 (VGLUT1) in postnatal development and control of quantal size. *Proceedings of the National Academy of Sciences*. 2004;101(18):7158-7163. doi:10.1073/pnas.0401764101
34. Mi Z, Abrahamson EE, Ryu AY, et al. Vesicular Glutamate Transporter Changes in the Cortical Default Mode Network During the Clinical and Pathological Progression of Alzheimer's Disease. *Journal of Alzheimer's Disease*. 2023;94(1):227-246. doi:10.3233/JAD-221063
35. Kashani A, Betancur C, Giros B, Hirsch E, Mestikawy S El. Altered expression of vesicular glutamate transporters VGLUT1 and VGLUT2 in Parkinson disease. *Neurobiol Aging*. 2007;28(4):568-578. doi:10.1016/j.neurobiolaging.2006.02.010
36. Guatteo E, Rizzo FR, Federici M, et al. Functional alterations of the dopaminergic and glutamatergic systems in spontaneous α-synuclein overexpressing rats. *Exp Neurol*. 2017;287:21-33. doi:10.1016/j.expneurol.2016.10.009
37. Barcomb K, Ford CP. Alterations in neurotransmitter co-release in Parkinson's disease. *Exp Neurol*. 2023;370:114562. doi:10.1016/j.expneurol.2023.114562
38. Saba L, Viscomi MT, Caioli S, et al. Altered Functionality, Morphology, and Vesicular Glutamate Transporter Expression of Cortical Motor Neurons from a Presymptomatic Mouse Model of Amyotrophic Lateral Sclerosis. *Cerebral Cortex*. 2016;26(4):1512-1528. doi:10.1093/cercor/bhu317
39. Namburi P, Beyeler A, Yorozu S, et al. A circuit mechanism for differentiating positive and negative associations. *Nature*. 2015;520(7549):675-678. doi:10.1038/nature14366
40. Okuyama T, Kitamura T, Roy DS, Itohara S, Tonegawa S. Ventral CA1 neurons store social memory. *Science (1979)*. 2016;353(6307):1536-1541. doi:10.1126/science.aaf7003
41. Amadei EA, Johnson Z V., Jun Kwon Y, et al. Dynamic corticostriatal activity biases social bonding in monogamous female prairie voles. *Nature*. 2017;546(7657):297-301. doi:10.1038/nature22381
42. Neumann ID, Slattery DA. Oxytocin in General Anxiety and Social Fear: A Translational Approach. *Biol Psychiatry*. 2016;79(3):213-221. doi:10.1016/j.biopsych.2015.06.004
43. Erskine D, Patterson L, Alexandris A, et al. Regional levels of physiological α-synuclein are directly associated with Lewy body pathology. *Acta Neuropathol*. 2018;135(1):153-154. doi:10.1007/s00401-017-1787-6
44. Vasili E, Dominguez-Meijide A, Flores-León M, et al. Endogenous Levels of Alpha-Synuclein Modulate Seeding and Aggregation in Cultured Cells. *Mol Neurobiol*. 2022;59(2):1273-1284. doi:10.1007/s12035-021-02713-2
45. Chen L, Nagaraja C, Daniels S, et al. Synaptic location is a determinant of the detrimental effects of α-synuclein pathology to glutamatergic transmission in the basolateral amygdala. *Elife*. 2022;11. doi:10.7554/eLife.78055
46. Bellingacci L, Sciaccaluga M, Megaro A, et al. Oligomeric alpha-synuclein causes early synaptic dysfunction of the corticostriatal pathway associated with non-motor symptoms. *NPJ Parkinsons Dis*. 2025;11(1):220. doi:10.1038/s41531-025-01075-z
47. Wu Q, Takano H, Riddle DM, Trojanowski JQ, Coulter DA, Lee VMY. α-Synuclein (αSyn) Preformed Fibrils Induce Endogenous αSyn Aggregation, Compromise Synaptic Activity and Enhance Synapse Loss in Cultured Excitatory Hippocampal Neurons. *The Journal of Neuroscience*. 2019;39(26):5080-5094. doi:10.1523/JNEUROSCI.0060-19.2019

ARTICLE IN PRESS

48. Jabra S, Rietsche M, Muellerleile J, et al. Sex- and cycle-dependent changes in spine density and size in hippocampal CA2 neurons. *Sci Rep*. 2024;14(1):12252. doi:10.1038/s41598-024-62951-x
49. Béïque J, Andrade R. PSD-95 regulates synaptic transmission and plasticity in rat cerebral cortex. *J Physiol*. 2003;546(3):859-867. doi:10.1113/jphysiol.2002.031369
50. Volpicelli-Daley LA, Luk KC, Patel TP, et al. Exogenous α-Synuclein Fibrils Induce Lewy Body Pathology Leading to Synaptic Dysfunction and Neuron Death. *Neuron*. 2011;72(1):57-71. doi:10.1016/j.neuron.2011.08.033
51. Shipton OA, Paulsen O. GluN2A and GluN2B subunit-containing NMDA receptors in hippocampal plasticity. *Philosophical Transactions of the Royal Society B: Biological Sciences*. 2014;369(1633):20130163. doi:10.1098/rstb.2013.0163
52. Bromberg-Martin ES, Matsumoto M, Hikosaka O. Dopamine in Motivational Control: Rewarding, Aversive, and Alerting. *Neuron*. 2010;68(5):815-834. doi:10.1016/j.neuron.2010.11.022
53. Wise RA, Spindler J, deWit H, Gerberg GJ. Neuroleptic-Induced "Anhedonia" in Rats: Pimozide Blocks Reward Quality of Food. *Science (1979)*. 1978;201(4352):262-264. doi:10.1126/science.566469
54. Eisenegger C, Pedroni A, Rieskamp J, et al. DAT1 Polymorphism Determines L-DOPA Effects on Learning about Others' Prosociality. *PLoS One*. 2013;8(7):e67820. doi:10.1371/journal.pone.0067820
55. Kampe KKW, Frith CD, Dolan RJ, Frith U. Reward value of attractiveness and gaze. *Nature*. 2001;413(6856):589-589. doi:10.1038/35098149
56. Eddy CM, Cook JL. Emotions in action: The relationship between motor function and social cognition across multiple clinical populations. *Prog Neuropsychopharmacol Biol Psychiatry*. 2018;86:229-244. doi:10.1016/j.pnpbp.2018.05.021
57. Chong TTJ, Husain M. The role of dopamine in the pathophysiology and treatment of apathy. In: 2016:389-426. doi:10.1016/bs.pbr.2016.05.007
58. Servillo F, De Carluccio M, Di Lazzaro G, et al. Molecular and cellular determinants of L-Dopa-induced dyskinesia in Parkinson's Disease. *NPJ Parkinsons Dis*. 2024;10(1):228. doi:10.1038/s41531-024-00836-6
59. Seibenhener ML, Wooten MC. Use of the Open Field Maze to measure locomotor and anxiety-like behavior in mice. *J Vis Exp*. 2015;(96):e52434. doi:10.3791/52434
60. Rodo C, Sargolini F, Save E. Processing of spatial and non-spatial information in rats with lesions of the medial and lateral entorhinal cortex: Environmental complexity matters. *Behavioural Brain Research*. 2017;320:200-209. doi:10.1016/j.bbr.2016.12.009
61. De Leonibus E, Pascucci T, Lopez S, Oliverio A, Amalric M, Mele A. Spatial deficits in a mouse model of Parkinson disease. *Psychopharmacology (Berl)*. 2007;194(4):517-525. doi:10.1007/s00213-007-0862-4
62. De Leonibus E, Managò F, Giordani F, et al. Metabotropic Glutamate Receptors 5 Blockade Reverses Spatial Memory Deficits in a Mouse Model of Parkinson's Disease. *Neuropsychopharmacology*. 2009;34(3):729-738. doi:10.1038/npp.2008.129
63. Giordano N, Iemolo A, Mancini M, et al. Motor learning and metaplasticity in striatal neurons: relevance for Parkinson's disease. *Brain*. 2018;141(2):505-520. doi:10.1093/brain/awx351
64. Golden SA, Covington HE, Berton O, Russo SJ. A standardized protocol for repeated social defeat stress in mice. *Nat Protoc*. 2011;6(8):1183-1191. doi:10.1038/nprot.2011.361

ARTICLE IN PRESS

ARTICLE IN PRESS

65. Verheggen FJ, Haubruge E, Mescher MC. Alarm Pheromones—Chemical Signaling in Response to Danger. In: 2010:215-239. doi:10.1016/S0083-6729(10)83009-2
66. Massaro Cenere M, Tiberi M, Paldino E, et al. Systemic inflammation accelerates neurodegeneration in a rat model of Parkinson's disease overexpressing human alpha synuclein. *NPJ Parkinsons Dis*. 2024;10(1):213. doi:10.1038/s41531-024-00824-w
67. Win-Shwe TT, Kyi-Tha-Thu C, Fujitani Y, Tsukahara S, Hirano S. Perinatal Exposure to Diesel Exhaust-Origin Secondary Organic Aerosol Induces Autism-Like Behavior in Rats. *Int J Mol Sci*. 2021;22(2):538. doi:10.3390/ijms22020538
68. Servillo F, De Carluccio M, Di Lazzaro G, et al. Molecular and cellular determinants of L-Dopa-induced dyskinesia in Parkinson's Disease. *NPJ Parkinsons Dis*. 2024;10(1):228. doi:10.1038/s41531-024-00836-6
69. Campanelli F, Marino G, Barsotti N, et al. Serotonin drives striatal synaptic plasticity in a sex-related manner. *Neurobiol Dis*. 2021;158. doi:10.1016/j.nbd.2021.105448
70. Mineo D, Cacace F, Mancini M, et al. Dopamine drives binge-like consumption of a palatable food in experimental Parkinsonism. *Movement Disorders*. 2019;34(6):821-831. doi:10.1002/mds.27683

ARTICLE IN PRESS

ARTICLE IN PRESS

Figures

ARTICLE IN PRESS

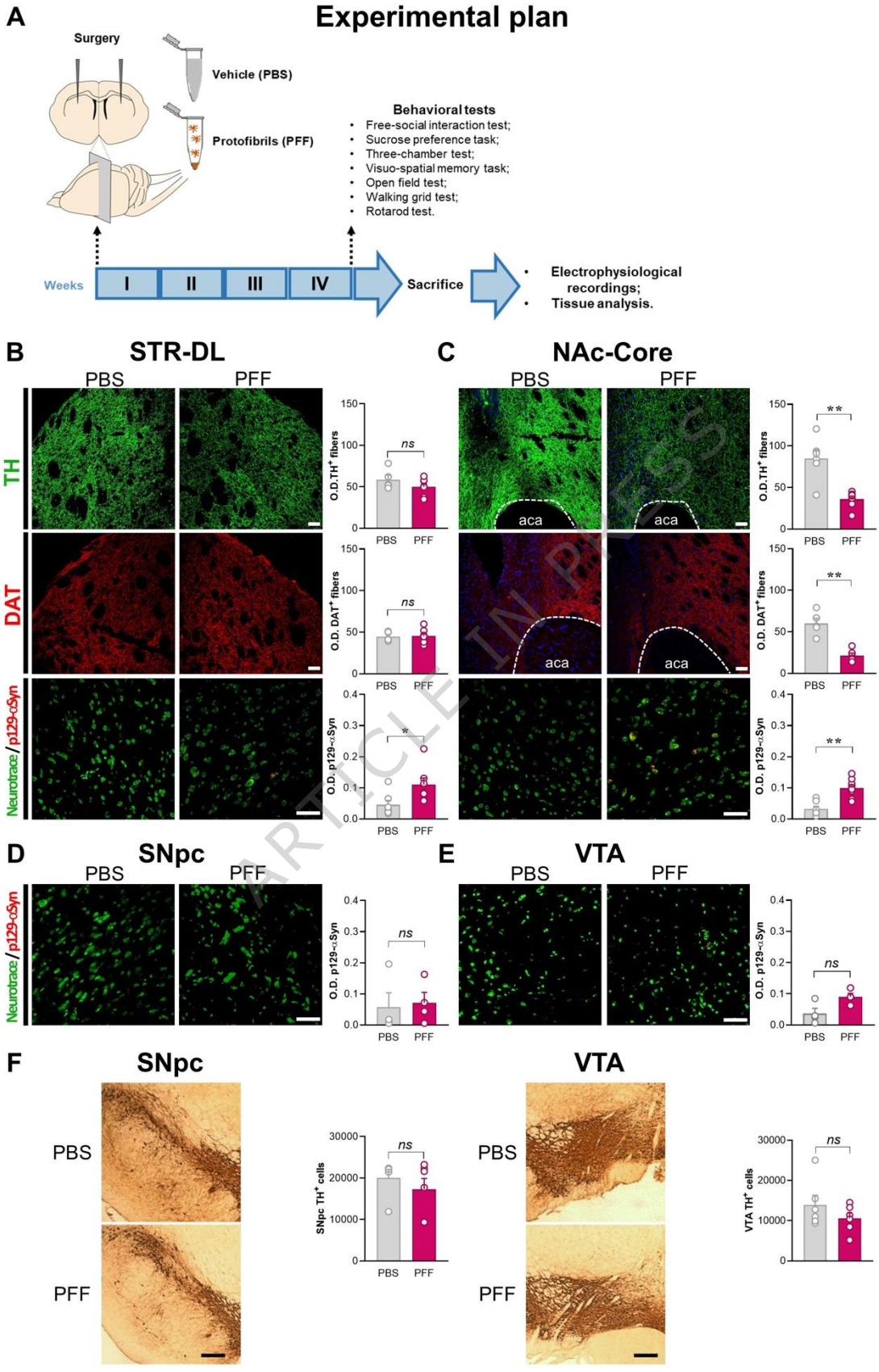
A
Experimental plan
Surgery
Vehicle (PBS)
Protofibrils (PFF)
Behavioral tests
Free-social interaction test;
Sucrose preference task;
Three-chamber test;
Visuo-spatial memory task;
Open field test;
Walking grid test;
Rotarod test.
Weeks
I
II
III
IV
Sacrifice
Electrophysiological recordings;
Tissue analysis.
B
STR-DL
C
NAc-Core
PBS
PFF
TH
DAT
Neurotrace / p129-αSyn
aca
O.D. TH+ fibers
O.D. DAT+ fibers
O.D. p129-αSyn
ns
*
**
D
SNpc
E
VTA
F
SNpc
VTA
SNpc TH+ cells
VTA TH+ cells

ARTICLE IN PRESS

Fig. 1. Schematic representation of the experimental timeline and morphological analysis of the dopaminergic pathways.
(A) Experimental plan: rats were bilaterally injected with PBS or α-syn-PFFs and, after four weeks, were subjected to motor and cognitive behavioral tests and then used for electrophysiological, immunofluorescence, and other morphological experiments. (B) Representative immunofluorescence images (left) and graphs (right) show TH ($P > 0.05$, *ns*), DAT ($P > 0.05$, *ns*), and p129-αSyn optical density (O.D.) (p129-αSyn *$P < 0.05$, PBS *versus* PFF) in the DL-STR from both experimental groups. (C) On the left side, immunofluorescence images are reported, and on the right side, the relative O.D. quantification graphs of TH (**$P < 0.01$, PBS *versus* PFF), DAT (**$P < 0.01$, PBS *versus* PFF), and p129-αSyn O.D. (**$P < 0.01$, PBS *versus* PFF) in NAc-Core from PBS and PFF groups. From the top to the bottom, scale bars are 50 μm, 50 μm, and 25 μm, respectively. In (D) and (E) are reported images (left) and relative O.D. quantification graphs (right) of p129-αSyn in the SNpc (ns $P > 0.5$) and in the VTA (ns $P > 0.05$), respectively. Scale bar, 25 μm. (F) Coronal brain sections in PBS and PFF groups show the number of TH^+ neurons with the TH immunoreactivity in the SNpc (left) and VTA (right). Scale bar, 200 μm. All the immunofluorescence images that report p129-αSyn immunofluorescence show p129-αSyn in red and the Neurotrace in green.

ARTICLE IN PRESS

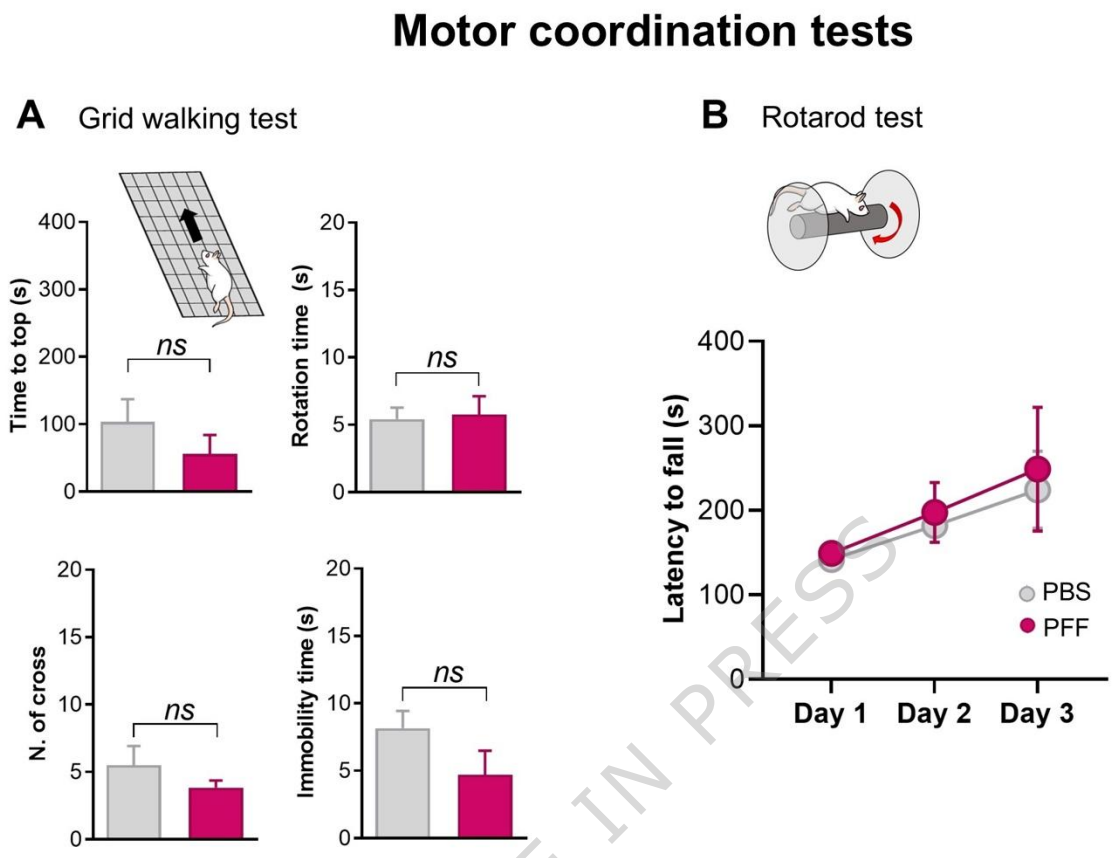

Fig. 2. Assessment of motor coordination and balance in PBS and α-syn-PFFs-injected groups.

(A) The histograms show averaged values of time to top (s), rotation time (s), number of crosses, and immobility time (s) in rats injected with PBS or α-syn-PFFs subjected to the Grid walking test (ns, $P > 0.5$). (B) The graph illustrates the performance in the Rotarod test in PBS or PFF groups, across trials of each day (ns, $P > 0.5$). Values are represented as means ± SEM. See the Methods section for details on behavioral procedures.

ARTICLE IN PRESS

Cognitive behavioral tests

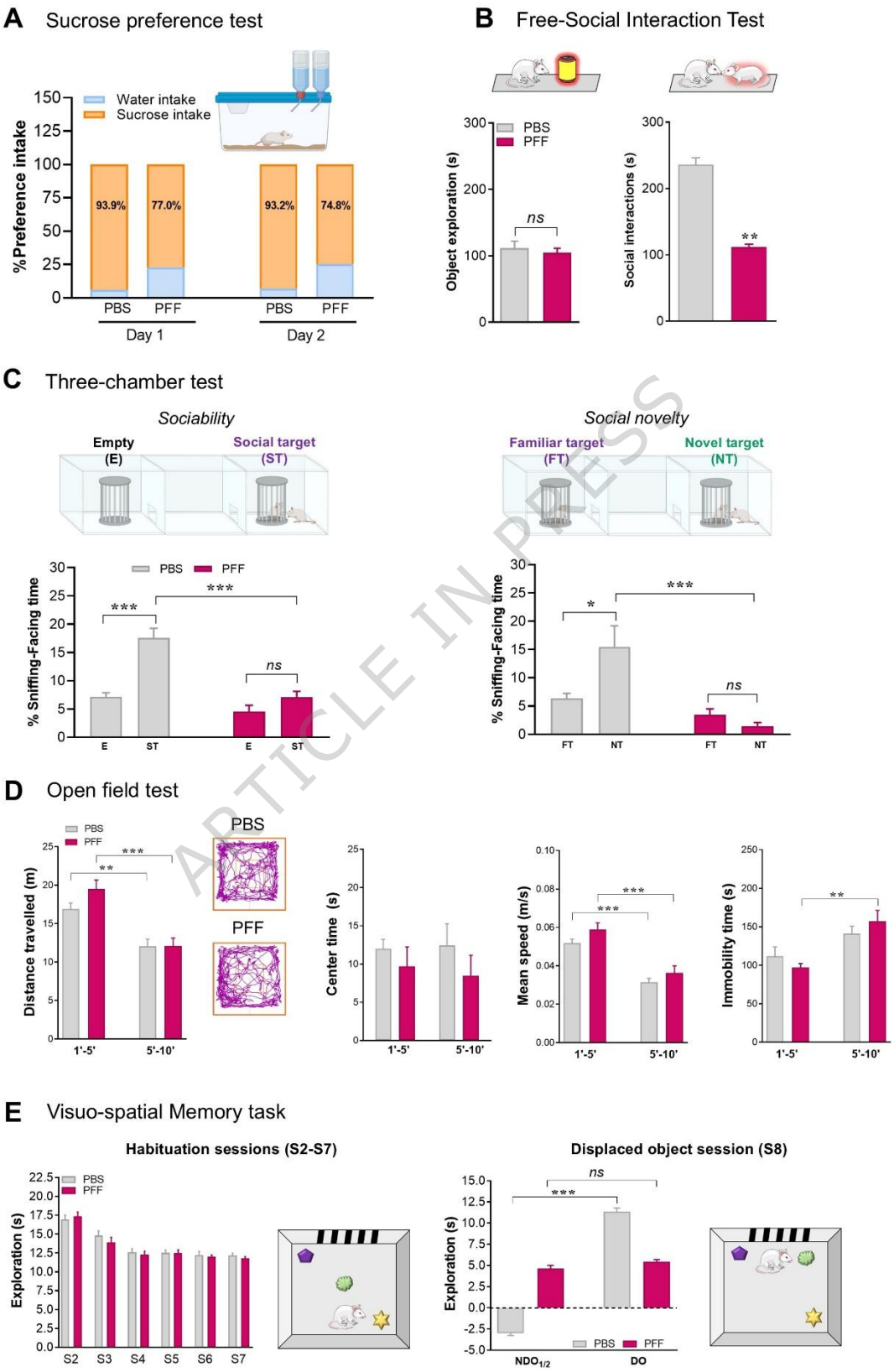

ARTICLE IN PRESS

ARTICLE IN PRESS

Fig. 3. Evaluation of cognitive deficits in PBS and α-syn-PFFs-injected animals.

(A) Sucrose preference test in PBS and PFF groups. Preference intake is reported as the percentage of sucrose (orange) and water (light blue) intake over total fluid consumption ($P > 0.05$). (B) Graphs show the free-social interaction of PBS and α-syn-PFFs-injected rats in the exploration time of the object (left) and approach (right) with a conspecific rat (**$P < 0.01$, PBS *versus* PFF). (C) Three-chamber test values are reported as percentages of sniffing-facing time. Graph in the left shows the sociability session (PBS: E *versus* ST, ***$P < 0.001$ and ST: PBS *versus* PFF, ***$P < 0.001$; PFF: E *versus* ST, $P > 0.05$), while graph on the right presents the preference for social novelty (PBS: FT *versus* NT, *$P < 0.05$, and NT: PBS *versus* PFF, ***$P < 0.001$; PFF: FT *versus* NT, $P > 0.05$). ST = social target, E = empty, FT = familiar target, NT = novel target. (D) The graphs show the activity in the visuo-spatial memory task. Left: The histogram displays the time (s) of object exploration during the habituation phase in the two experimental groups. Right: Graph indicates the exploration time (s) spent exploring a DO and NDOs during the session of spatial displacement. Schematic representations of the visuo-spatial memory task are reported to the right of the respective graphs [***$P < 0.001$, PBS (NDO1/2) *versus* PBS (DO)]. (E) The histograms show measurements of the distance traveled (m) (**$P < 0.01$, PBS; ***$P < 0.001$, PFF), time spent in the center (s), mean speed (m/s) (***$P < 0.001$, PBS; ***$P < 0.001$, PFF), and immobility time (s) (**$P < 0.01$, PFF) in PBS and PFF rats during the open field test. Representative plots of the trajectory traveled by PBS and PFF rats are shown in the upper part. Values are represented as means ± SEM. See the Methods section for details on behavioral procedures.

ARTICLE IN PRESS

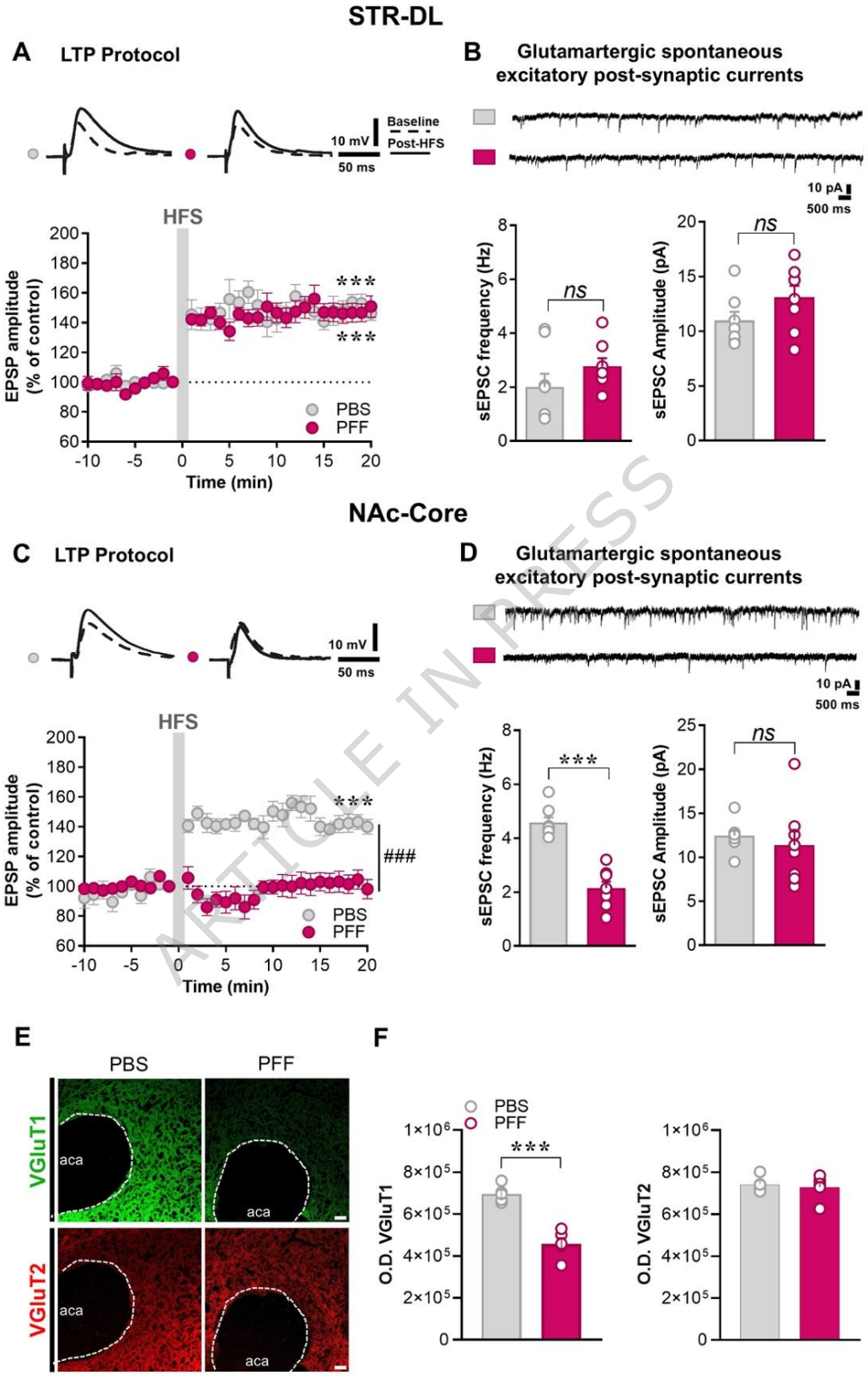
STR-DL
A
LTP Protocol
10 mV
50 ms
Baseline
Post-HFS
HFS
EPSP amplitude (% of control)
Time (min)
PBS
PFF
***
***
B
Glutamartergic spontaneous excitatory post-synaptic currents
10 pA
500 ms
sEPSC frequency (Hz)
sEPSC Amplitude (pA)
ns
ns
NAc-Core
C
LTP Protocol
10 mV
50 ms
HFS
EPSP amplitude (% of control)
Time (min)
PBS
PFF
***
###
D
Glutamartergic spontaneous excitatory post-synaptic currents
10 pA
500 ms
sEPSC frequency (Hz)
sEPSC Amplitude (pA)
***
ns
E
PBS
PFF
VGluT1
VGluT2
aca
aca
aca
aca
F
PBS
PFF
O.D. VGluT1
O.D. VGluT2
***

ARTICLE IN PRESS

Fig. 4. Functional synaptic plasticity in SPNs of PBS and PFF animals in STR-DL and NAc-Core regions.

(A) Time course of EPSP amplitude in SPNs recorded in STR-DL in response to LTP protocol after the application of HFS, from PBS or PFF-injected rats. Top: representative traces of single SPNs recorded in STR-DL of both groups before (dashed lines) and after (solid lines) HFS. (B) Frequency and amplitude of sEPSCs recorded from STR-DL SPNs of PBS or PFF-injected groups. (C) Time course of EPSP amplitude in SPNs recorded in NAc-Core in response to LTP protocol after the application of a tetanic stimulation, from PBS or PFF-injected rats ($^{###}P < 0.001$, PBS *versus* PFF). Top: representative traces of single SPNs recorded in NAc-Core of PBS and PFF groups before (dashed lines) and after (solid lines) HFS. Scale bars, 50 ms/10 mV. (D) Measurement of frequency (***$P < 0.001$, PBS *versus* PFF) and amplitude of sEPSCs, recorded from corticostriatal rat slices of both experimental groups in NAc-Core SPNs. (E) Representative images show VGluT1 (green) and VGluT2 (red) in the NAc-Core from PBS and PFF groups. (F) Histograms report the O.D. of VGluT1 and VGluT2 in the NAc-Core (VGluT1: ***$P < 0.001$, PBS *versus* PFF; VGluT2: $P < 0.05$, PBS *versus* PFF); aca: anterior commissure. Scale bars = 50 μm.

ARTICLE IN PRESS

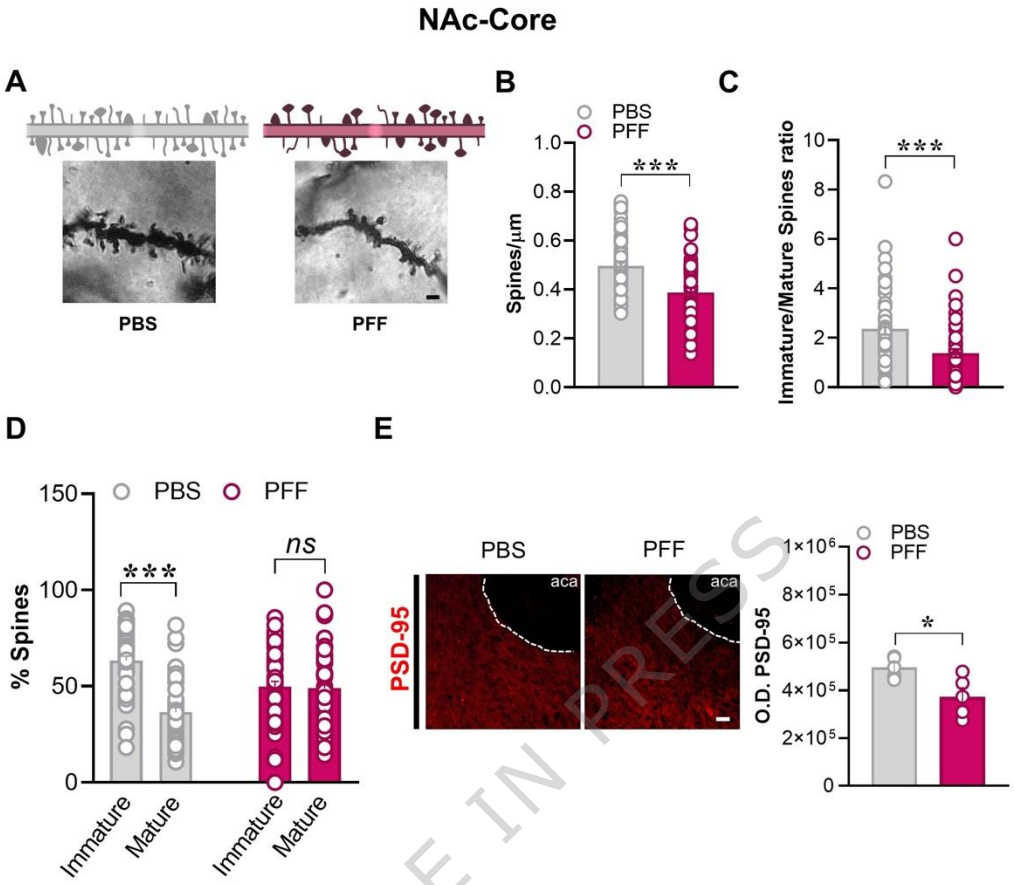

Fig.5 Structural SPNs changes in dendritic spines in the NAc-Core α-syn-PFFs.
(A) Representative images of Golgi-stained dendritic spines of NAc-Core SPNs in both groups after striatal injection of PBS or α-syn-PFFs. Scale bar, 250 µm. (B-C) Histograms show the quantification of dendritic spine density (Spines/µm) (***P < 0.001, PBS *versus* PFF, left) and the immature/mature spines ratio (***P < 0.001, PBS *versus* PFF, right). (D) The percentage of the total number of spines immature and mature between PBS and PFF groups (***P < 0.001, PBS Immature *versus* PBS Mature). (E) On the left, representative images show PSD-95 (Red) in the NAc-Core close to the anterior commissure (aca) from PBS and PFF groups. On the right, the histogram reports the O.D. of PSD-95 in the NAc-Core (O.D. PSD-95: *P < 0.05, PBS *versus* PFF). Scale bars = 50 µm.

ARTICLE IN PRESS

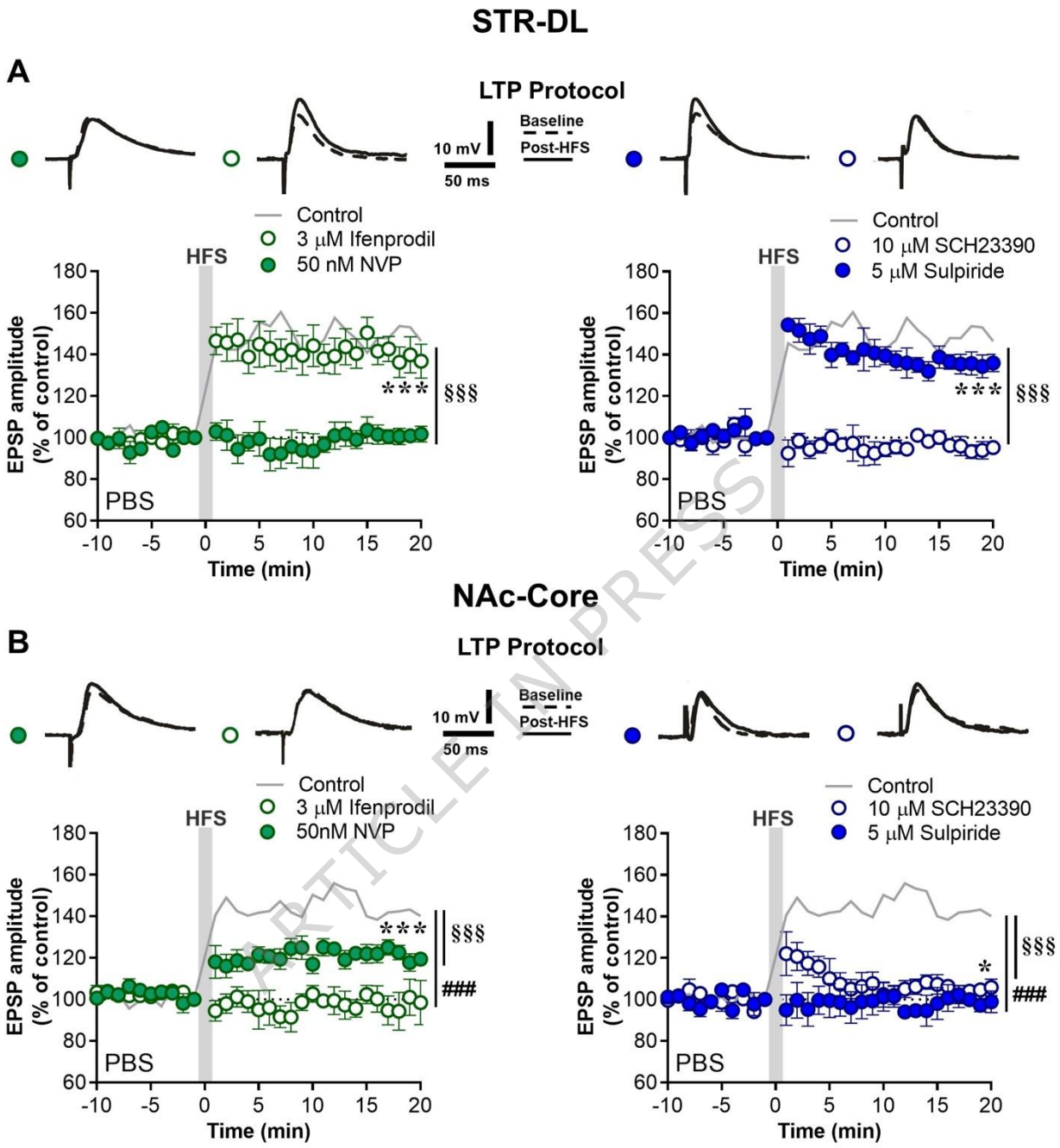

Fig. 6. Pharmacological manipulation of LTP in STR-DL in normal conditions and NAc-Core.

(A) Time course of LTP in STR-DL SPNs from the PBS animals, recorded in physiological condition (gray solid line) and after 10 min bath application of (left) NMDAR (NVP 50 nM, and ifenprodil 3 μM) and (right) DAR antagonists (SCH-23390 10 μM, and sulpiride 5 μM) ($^{§§§}P < 0.001$, PBS + NVP 50 nM *versus* Control and PBS + SCH-23390 10 μM *versus* Control; ***P < 0.001, PBS + ifenprodil 3 μM pre- *versus* 20 min post-HFS and PBS + sulpiride 5 μM pre- *versus*

ARTICLE IN PRESS

20 min post-HFS). Scale bars, 10 ms/50 mV. Top: representative traces of SPNs EPSPs recorded from PBS rats before (dashed lines) and after (solid lines) HFS. (B) Time course of LTP in NAc-Core SPNs from the PBS animals, recorded in physiological condition (gray solid line) and after 10 min bath application of NMDAR (left) and DAR (right) antagonists. ($^{§§§}P < 0.001$, Control versus PBS + NVP 50 nM, and $^{###}P < 0.001$, Control *versus* PBS + ifenprodil 3 μM; $^{§§§}P < 0.001$, Control *versus* PBS + SCH-23390 10 μM, and $^{###}P < 0.001$, Control *versus* PBS + sulpiride 5 μM; ***$P < 0.001$, PBS + NVP 50 nM pre- *versus* 20 min post-HFS and *$P < 0.05$, PBS + SCH-23390 10 μM pre- *versus* 20 min post-HFS). Scale bars, 10 ms/50 mV. Top: representative traces of SPNs EPSPs recorded from PBS rats before (dashed lines) and after (solid lines) HFS.

ARTICLE IN PRESS

Sub-chronic L-Dopa treatment

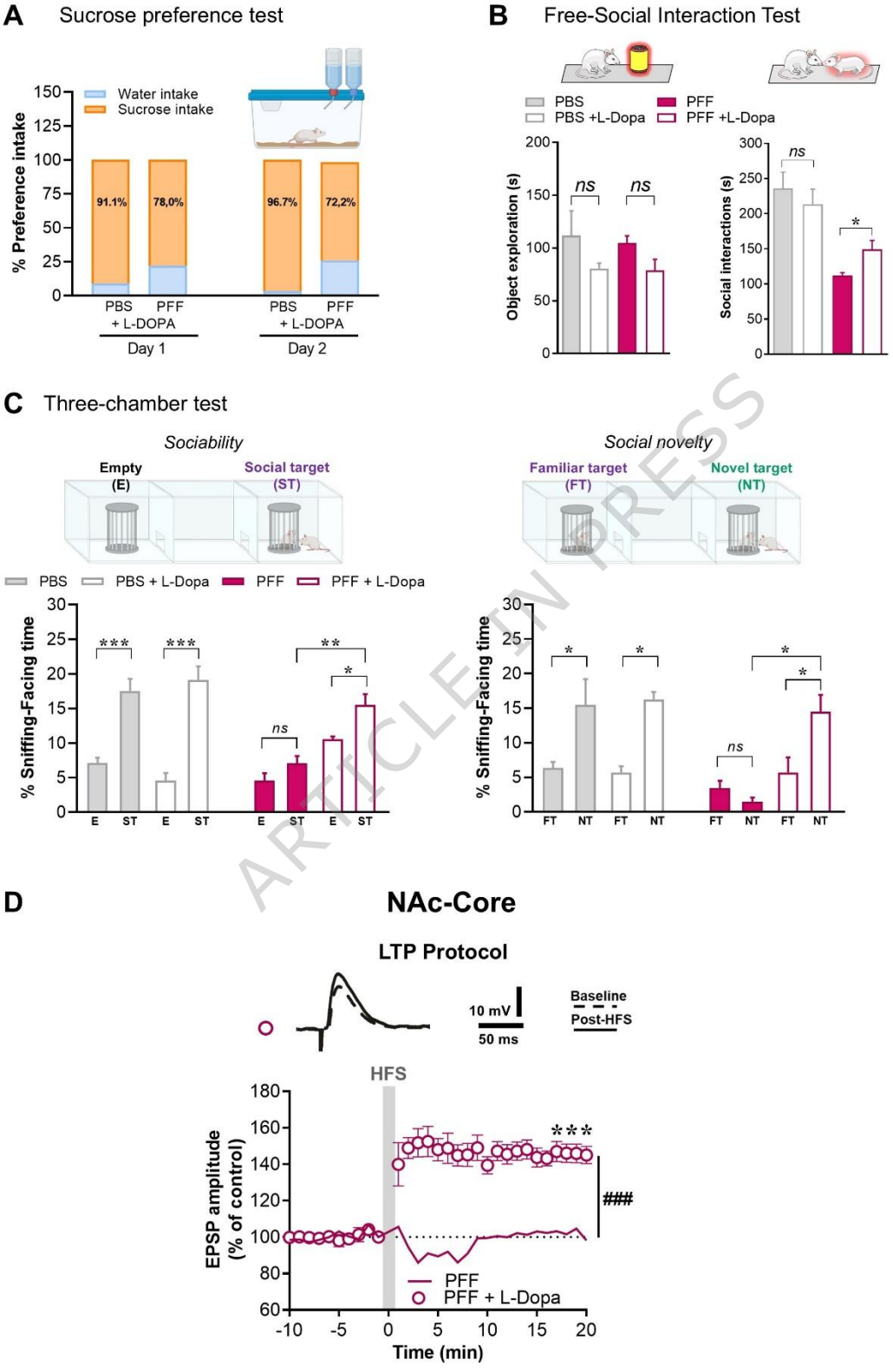

ARTICLE IN PRESS

ARTICLE IN PRESS

Fig. 7. L-Dopa treatment ameliorates cognitive impairments and synaptic dysfunction induced by α-syn-PFFs injection in rats.
(A) Sucrose preference test in both L-Dopa–treated experimental groups. The preference for sucrose is expressed as the percentage of sucrose (orange) and water (light blue) intake relative to the total fluid consumption ($P > 0.05$). (B) Graphs illustrate the free social interaction of PBS- and α-syn-PFF–injected rats treated with or without L-Dopa, expressed as exploration time of the object (left) and approach behavior (right) (object exploration: *ns*, $P > 0.05$, PBS *versus* PBS + L-Dopa and PFF *versus* PFF + L-Dopa; social interaction: *ns*, $P > 0.05$, PBS *versus* PBS + L-Dopa and $^{*}P < 0.05$, PFF *versus* PFF + L-Dopa). (C) Three-chamber test in all experimental groups. Left: sociability session, (PBS + L-Dopa: $^{***}P < 0.001$ and PFF + L-Dopa: $^{*}P < 0.05$, E *versus* ST; ST: PFF *versus* PFF + L-Dopa: $^{**}P < 0.01$ and). Right: social novelty (PBS + L-Dopa: $^{*}P < 0.05$ and PFF + L-Dopa: $^{*}P < 0.05$, FT *versus* ST and NT: PFF *versus* PFF + L-Dopa: $^{*}P < 0.05$). (D) Time course of LTP in NAc-Core SPNs before and 20 min after the HFS protocol in PFF (line) and PFF + L-Dopa animals at 4 weeks from injection ($^{\#\#\#}P < 0.001$, PFF *versus* PFF + L-Dopa). Scale bar = 10 mV, 50 ms.

ARTICLE IN PRESS